Electronic Supplementary Material (ESI) for ChemComm.

Supporting Information

Tuning of the flexibility in metal-organic frameworks based on pendant arm macrocycles

Sungeun Jeoung,[a] Songho Lee,[a] Jae Hwa Lee,[a] Soochan Lee,[b] Wonyoung Choe,[b] Dohyun Moon,*[c] and Hoi Ri Moon*[a]

[a] Department of Chemistry, Ulsan National Institute of Science and Technology (UNIST), 50 UNIST-gil, Ulsan 44919, Republic of Korea

[b] Department of Chemistry, Ulsan National Institute of Science and Technology (UNIST), 50 UNIST-gil, Ulsan 44919, Republic of Korea

[c] Beamline Division, Pohang Accelerator Laboratory, 80 Jigok-ro, 127beon-gil, Nam-gu, Pohang, Gyeongbuk 37673, Republic of Korea

* e-mail: hoirimoon@unist.ac.kr; dmoon@postech.ac.kr

Experimental Section

Materials and methods. All chemicals and solvents used in the syntheses were of reagent grade and they were used without further purification. 2,2',5,5'-tetramethylbiphenyl, 98% bought from Alfa Aesar and 2,2',5,5'-biphenyltetracarboxylic acid (H_4BPTC) was prepared according to the method previously reported.[S1] $[Ni(C_{14}H_{28}N_8)]Cl_2$ ($[NiL_{CN}]Cl_2$), $[Ni(C_{12}H_{30}N_6O_2)](ClO_4)_2$ ($[NiL_{OH}](ClO_4)_2$), and $[Ni(C_{14}H_{30}N_6)](ClO_4)_2$ ($[NiL_{CH2}](ClO_4)_2$) were prepared by the reported methods with a modification.[S2] Infrared spectra were measured by a Thermo Fisher Scientific Nicolet 6700 FT-IR spectrometer. X-ray powder diffraction (XRPD) data were recorded on a Bruker D2 phaser diffractometer at 30 kV and 10 mA for Cu Kα (λ = 1.54050 Å), with a step size of 0.02º in 2θ. N_2, CO_2, H_2O sorption isotherms of samples were obtained using a BELSORP-max at 77 K, 196 K, and 298 K, respectively. Prior to the adsorption measurements, the samples were evacuated ($p < 10^{-5}$ mbar) at RT for 24 h and then 110 °C for 4 h. Thermogravimetric analysis (TGA) were performed under N_2(g) atmosphere at a scan rate of 5 ^oC/min using Q50 from TA instruments. Elemental analyses were done by UNIST Central Research Facilities center (UCRF) in Ulsan National Institute of Science and Technology (UNIST).

Synthesis of $[(Ni(C_{14}H_{28}N_8)]Cl_2$ ($[NiL_{CN}]Cl_2$). To a stirred methanol solution (50 mL) of $NiCl_2 \cdot 6H_2O$ (11.9 g) were slowly added ethylenediamine (6.8 mL) at 0 ^oC, and then paraformaldehyde (7.5 g), 3-aminopropaneitrile (10 mL) was added in ordered referred. The residual mixture was sufficiently stirred at room temperature for about 30 min. Then, it was refluxed for 24 h. After it was cool down at RT, the mixture was filtered, and pale purple powder was washed with methanol, and dried at room temperature under vacuum. The pale

purple powder was recrystallized by using at methanol 30 mL and at least H_2O in heating water bath at 100 °C, then crystal grows as it cool down, filtered it, washed MeOH, and dried at room temperature under vacuum. Anal. Calcd for $Ni_1C_{14}H_{28}N_8Cl_2$: C, 37.06; H, 6.80; N, 26.01.; Found: C, 38.38; H, 6.44; N, 25.58. FT-IR for $[NiL_{CN}]Cl_2$ (ATR) : υ_{H2O} 3500 , $\upsilon_{C\equiv N}$ 2248 cm^{-1}, υ_{C-H} 2955, 2919 cm^{-1}.

Synthesis of $[(Ni(C_{12}H_{30}N_6O_2)](ClO_4)_2$ ($[NiL_{OH}](ClO_4)_2$). To a stirred methanol solution (50 mL) of $NiCl_2{\cdot}6H_2O$ (11.9 g) were slowly added ethylenediamine (6.8 mL) at 0 °C, and then paraformaldehyde (7.5 g), ethanolamine (8.7 mL) was added in ordered referred. The residual mixture was sufficiently stirred at room temperature for about 30 min. Then, it was refluxed for 6 h. After it was cool down at r.t., the mixture was filtered, and purple powder was washed with methanol, and dried at room temperature under vacuum. It was dissolved in deionized water 250 mL with stirring, and then 70% perchloric acid 10 mL was slowly added to yellow solution at 0 °C. In addition, to provide excess anion, after sodium perchloroate (2.6 g) was added, store it at refrigerator for 1 day. Then, yellow powder was formed, which were filtered off, washed with methanol, and dried under vacuum. The yellow powder was recrystallized by using at least H_2O in heating water bath at 100 °C, then crystal grows as it cool down, filtered it, washed methanol, and dried at room temperature under vacuum. Anal. Calcd for $Ni_1C_{12}H_{30}N_6O_8Cl_2$: C, 26.30; H, 5.52; N, 15.33.; Found: C, 26.15; H, 5.40; N, 15.49. FT-IR for $[NiL_{OH}](ClO_4)_2$ (ATR) : υ_{O-H} 3572, $\upsilon_{N-H(secondary\ amine)}$ 3205, υ_{C-H} 2985, 2891, υ_{ClO4} 1060 cm^{-1}.

Synthesis of $[(Ni(C_{14}H_{30}N_6)](ClO_4)_2$ ($[NiL_{CH2}](ClO_4)_2$). To a stirred methanol solution (50 mL) of $NiCl_2{\cdot}6H_2O$ (11.9 g) were slowly added ethylenediamine (7.0 mL) at 0 °C, and then

paraformaldehyde (7.5 g), allylamine (8.4 mL) was added in ordered referred. The residual mixture was sufficiently stirred at room temperature for about 30 min. Then, it was refluxed for 12 h. After it was cool down at r.t., the mixture was filtered, and pale purple powder was washed with methanol, and dried at room temperature under vacuum. It was dissolved in deionized water 250 mL with stirring, and then 70% perchloric acid 10 mL was slowly added to yellow solution at 0 ^{o}C. In addition, to provide excess anion, after sodium perchloroate (2.6 g) was added, store it at refrigerator for 1 day. Then, yellow powder was formed, which were filtered off, washed with methanol, and dried under vacuum. The yellow powder was recrystallized by using at least H_2O/MeCN = 1:1 (v/v) in heating water bath at 100 ^{o}C, then crystal grows as it cool down, filtered it, washed methanol, and dried at room temperature under vacuum. Anal. Calcd for $NiC_{14}H_{30}N_6O_8Cl_2$: C, 31.13; H, 5.60; N, 15.56.; Found: C, 31.05; H, 5.98; N, 16.75. FT-IR for $[NiL_{CH2}](ClO_4)_2$ (ATR) : $\upsilon_{C=C}$ 1639, $\upsilon_{N\text{-}H(secondary\ amine)}$ 3201, $\upsilon_{C\text{-}H}$ 2965, 2891, υ_{ClO4} 1068 cm^{-1}.

Synthesis of {[(NiL$_{CN}$)$_2$(BPTC)]·4DMF·2H$_2$O} (*as-flex*MOF(CN)). $[NiL_{CN}]Cl_2$ (0.062 g, 0.035 mmol) and H_4BPTC (0.024 g, 0.070 mmol) were dissolved in mixture solution of *N,N*-dimethylformamide (DMF) and H_2O with volume ratio of 1.5 mL:1.5 mL and 2 mL:1 mL with TEA 80 μL respectively. The solution of H_4BPTC was added to the $[NiL_{CN}]Cl_2$ solution, mixed two solutions by voltex mixer, and allowed to stand at refrigerator for 7 days. Yield: ~23.5%. Anal. Calcd for $Ni_2C_{56}H_{94}N_{20}O_{14}$: C, 48.43; H, 6.82; N, 20.17.; Found: C, 48.44; H, 6.73; N, 20.10. FT-IR for ***as-flex*MOF(CN)** (ATR): $\nu_{C\equiv N}$ 2246, $\nu_{N\text{-}H(secondary\ amine)}$ 3154, $\nu_{C\text{-}H}$ 2926, 2869, $\nu_{COO\text{-}}$ 1572, 1381 cm^{-1}.

Preparation of activated *flex*MOF(CN) (*cp-flex*MOF(CN)). To activate ***as-flex*MOF(CN)**, the guest molecules were exchanged. The mother liquor containing crystals of as-synthesized ***as-flex*MOF(CN)** was decanted carefully by pipette, and the crystals were re-immersed in distilled MeCN for 3 days with refreshing the solvent 6 times. Then, the crystals were filtered and evacuated at RT for 24 h, and then 110 ^{o}C for 4 h under vacuum. Then, cooled the sample and refilled the gas with Ar.

Synthesis of {[(NiL_{OH})$_2$(BPTC)]·1DMF·3H_2O} (*as-flex*MOF(OH)). [NiL_{OH}](ClO_4)$_2$ (0.064 g, 0.014 mmol) and H_4BPTC (0.024 g, 0.070 mmol) were dissolved in mixture solution of *N,N*-dimethylformamide (DMF) and H_2O with volume ratio of 1.5 mL:1.5 mL and 2 mL:1 mL with TEA 80 μL respectively. The solution of H_4BPTC was added to the [NiL_{OH}](ClO_4)$_2$ solution, mixed two solutions by voltex mixer, and allowed to stand at refrigerator for 7 days. Yield: ~32%. Anal. Calcd for $Ni_2C_{43}H_{79}N_{13}O_{16}$: C, 44.85; H, 6.91; N, 15.81.; Found: C, 44.64; H, 6.94; N, 15.88. FT-IR for ***as-flex*MOF(OH)** (ATR): ν_{O-H} 3434, $\nu_{N-H(secondary\ amine)}$ 3154, ν_{C-H} 2926, 2869, ν_{COO-} 1571, 1354 cm^{-1}.

Preparation of activated *flex*MOF(OH) (*cp-flex*MOF(OH)). To activate ***as-flex*MOF(OH)**, the guest molecules were exchanged. The mother liquor containing crystals of as-synthesized ***as-flex*MOF(OH)** was decanted carefully by pipette, and the crystals were re-immersed in distilled THF for 3 days with refreshing the solvent 6 times. Then, the crystals were filtered and evacuated at RT for 24 h, and then 110 ^{o}C for 4 h under vacuum. Then, cooled the sample and refilled the gas with Ar.

Synthesis of {[(NiL_{CH2})$_2$(BPTC)]·1MeCN·5H_2O} (*as-flex*MOF(CH_2)). [NiL_{CH2}](ClO_4)$_2$ (0.078 g, 0.035 mmol) and H_4BPTC (0.024 g, 0.070 mmol) were dissolved in mixture solution of acetonitrile (MeCN) and H_2O with volume ratio of 2 mL:1 mL and 2 mL:1 mL with TEA 80 μL respectively. The solution of H_4BPTC was added to the [NiL_{CH2}](ClO_4)$_2$ solution, mixed two solutions by voltex mixer, and allowed to stand at room temperature for 7 days. Yield: ~40%. Anal. Calcd for $Ni_2C_{46}H_{79}N_{13}O_{13}$: C, 48.48; H, 6.99; N, 15.98.; Found: C, 48.48; H, 6.24; N, 16.01. FT-IR for ***as-flex*MOF(CH_2)** (ATR): $\nu_{N\text{-}H(secondary\ amine)}$ 3139, $\nu_{C\text{-}H}$ 2914, 2862, $\nu_{COO\text{-}}$ 1571, 1343 cm^{-1}.

Preparation of activated *flex*MOF(OH) (*cp-flex*MOF(CH_2)). To activate ***as-flex*MOF(CH_2)**, the guest molecules were exchanged. The mother liquor containing crystals of as-synthesized ***as-flex*MOF(CH_2)** was decanted carefully by pipette, and the crystals were re-immersed in distilled MeCN for 3 days with refreshing the solvent 6 times. Then, the crystals were filtered and evacuated at RT for 24 h, and then 110 ^oC for 4 h under vacuum. Then, cooled the sample and refilled the gas with Ar.

Synchrotron X-ray Powder Diffraction (XRPD) measurement. The diffraction data were measured with transmission-mode as Debye-Scherrer Pattern with the 100 mm of sample-to-detector distance in 40 s exposure on a Rayonix MX225HS CCD detector at BL2D SMC with a silicon (111) double crystal monochromator (DCM) at the Pohang Accelerator Laboratory, Korea. In-situ variable pressure XRPD was measured with a custom-made vacuum manifold and goinometer head. The PAL BL2D-SMDC program[S3] was used for data collection, and the Fit2D[S4] program was used for conversion of integrated 2D to 1D patterns, for wavelength and

detector distance refinement and for a calibration measurement of a NIST Si 640c standard sample.

in-situ **synchrotron XRPD experiment.** The XRPD patterns of ***flex*****MOF(CN)**, ***flex*****MOF(OH)**, and ***flex*****MOF(CH_2)** were collected at 195 K with synchrotron radiation (λ = 1.20000 Å). The carbon dioxide gas was extra-high purity (DAEHAN Gas Company, Korea, 99.999%). To prepare the XPRD samples, the activated samples, ***cp-flex*****MOF(CN)**, ***cp-flex*****MOF(OH)**, and ***cp-flex*****MOF(CH_2)** were ground and packed into capillary (diameter, 0.3 mm; wall thickness, 0.01 mm) under Ar atmosphere in glove box. Prior to data collection sample was outgassed at 383 K under a primary vacuum until it did not reveal any significant the shift of XRPD pattern. Then, the sample was cooled to 196 K by using a cryostream under vacuum. To observe the structural transformation induced by adsorbing CO_2 gas, the diffraction patterns were measured with applying various pressure of CO_2 gas to capillary at 196 K. The XRPD patterns during adsorption of CO_2 were sequentially collected at 0, 0.20, 0.40, 0.60, 0.80, and 0.98 atm, and for desorption measurement at 0.80, 0.60, 0.40, 0.20, and 0 atm by using fine adjustable manual needle valve. After 20 min from applying each pressure to the sample, the patterns were collected during adsorption measurement.

Single-Crystal X-ray crystallography. Single-crystals were coated with Parabar 10312 (Hampton Research Inc.) to mount micro-loop. The Single Crystal X-ray diffraction data measured using synchrotron employing a PLSII-2D SMC an ADSC Quantum-210 detector for dried crystal and Rayonix MX225HS for as-synthesized crystals, respectively, with a silicon (111) double crystal monochromator (DCM) at Pohang Accelerator Laboratory, Korea. The

PAL BL2D-SMDC program[S3] was used for both data collection, and HKL3000sm (Ver. 730r)[S5] was used for cell refinement, reduction and absorption correction. The crystal structures were solved by the intrinsic phasing method with SHELX-XT (Ver. 2018/2),[S6] and refined by full-matrix least-squares calculation with SHELX-XL (Ver. 2018/3).[S7] All non-hydrogen atoms in whole structures were refined anisotropically. Although some structure solvents were observed by Fourier Maps in the X-ray diffraction, the exact position of these solvent molecules could not be well defined due to disordered solvent of diffused electron densities. Using the SQUEEZE routine in the software of PLATON,[S8] we performed the final structure refinements. For ***as-flex*MOF(CN)**, the solvent accessible volume is 4592 Å^3 (52.5%) for the unit cell, where 1251 electrons are found, equivalent to the electrons of ~31 DMF molecules or ~125 water molecules, or their combination. For ***cp-flex*MOF(CN)**, the solvent accessible volume is 153 Å^3 (6.10%) for the unit cell, where 36 electrons are found, equivalent to the electrons of ~3.5 water molecules. For ***as-flex*MOF(OH)**, the solvent accessible volume is 1312 Å^3 (36.7%) for the unit cell, where 378 electrons are found, equivalent to the electrons of ~9.5 DMF molecules or ~38 water molecules, or their combination. For ***cp-flex*MOF(OH)**, the solvent accessible volume is 158 Å^3 (6.63%) for the unit cell, where 19 electrons are found, equivalent to the electrons of ~2 water molecules. For ***as-flex*MOF(CH_2)**, the solvent accessible volume is 1600 Å^3 (25.2%) for the unit cell, where 536 electrons are found, equivalent to the electrons of ~13 DMF molecules or ~54 water molecules, or their combination. For ***cp-flex*MOF(CH_2)**, the solvent accessible volume is 92 Å^3 (3.88%) for the unit cell, where 20 electrons are found, equivalent to the electrons of ~2 water molecules. A summary of the crystals and some crystallographic data are given in Table S1 – S9. CCDC 1898507 (***as-flex*MOF(CN)**), 1898504 (***cp-flex*MOF(CN)**), 1898506 (***as-flex*MOF(OH)**), 1898505 (***cp-flex*MOF(OH)**), 1908259 (***as-flex*MOF(CH_2)**), and 1908261 (***cp-***

***flex*MOF(CH$_2$)**) contain the supplementary crystallographic data for this paper. The data can be obtained free of charge at www.ccdc.cam.ac.uk/conts/retrieving.html or from the Cambridge Crystallographic Data Centre, 12, Union Road, Cambridge CB2 EX, UK.

Grand Canonical Monte Carlo (GCMC) simulation. GCMC simulation of CO_2 adsorption at 196 K and 1 bar in ***as-flex*MOF(CN)** single-crystal structure was carried out using RASPA 2.0 code.[S9] The framework charge was not considered to neglect electrostatic interaction between framework atoms and adsorbate molecules. Simulation for CO_2 adsorption used 10,000-cycle for equilibration and 10,000-cycle for data collection. One cycle is composed of *N* Monte Carlo steps, where *N* is the number of adsorbate molecules in system. The Monte Carlo step included randomly insertion, deletion, translation, rotation, and reinsertion moves with equal probabilities.

The used intermolecular interactions, adsorbate-adsorbate and framework-adsorbate, were followed with Lennard-Jones and Coulomb potential,

$$V_{ij} = 4\varepsilon_{ij}\left[\left(\frac{\sigma_{ij}}{r_{ij}}\right)^{12} - \left(\frac{\sigma_{ij}}{r_{ij}}\right)^{6}\right] + \frac{q_i q_j}{4\pi\epsilon_0 r_{ij}}$$

where ε_{ij} is the Lennard-Jones potential-well depth; σ_{ij} is the Lennard-Jones hard-sphere model diameter; r_{ij} is the distance between i and j atoms; q_i and q_j are the partial charge of i and j atoms, respectively; ϵ_0 is the vacuum permittivity. All Lennard-Jones potentials were truncated as a cut-off radius of 12.8 Å.

The used forcefield for potential energy parameters on calculation was universal force field (UFF). TraPPE molecular forcefield was used in calculation for gas model.[S10] Lennard-Jones

potential energy parameters of CO_2 are shown in Table S10. GCMC CO_2 adsorption simulation result in ***as-flex*MOF(CN)** and ***as-flex*MOF(CH_2)** were summarized in Table S11.

Table S1. X-ray crystallographic data of ***as-flex*MOF(CN)** and ***cp-flex*MOF(CN)**.

Compound	***as-flex*MOF(CN)**	***cp-flex*MOF(CN)**
formula	$Ni_2C_{44}H_{62}N_{16}O_8$	$Ni_4C_{88}H_{124}N_{32}O_{16}$
crystal system	*Monoclinic*	*Triclinic*
space group	*C*2/*c*	*P*-1
fw	1060.51	2121.02
a, Å	21.799(4)	10.063(2)
b, Å	25.727(5)	15.927(3)
c, Å	15.630(3)	16.581(3)
α, deg	90	86.837(8)
β, deg	93.86(3)	74.753(5)
γ, deg	90	78.205(9)
V, Å^3	8746(3)	2509.8(8)
Z	4	1
ρ_{calcd}, g cm^{-3}	0.805	1.403
temp , K	220(2)	100(2)
λ, Å	0.700	0.700
μ, mm^{-1}	0.449	0.782
goodness-of-fit (F^2)	1.097	0.977
F(000)	2232	1116
reflections collected	35918	16553
independent reflections	9987 [*R*(int) = 0.0633]	8602 [*R*(int) = 0.0677]
completeness to θ_{max}, %	99.8%	93.2%
data/restraints/parameters	9987 / 6 / 319	8602 / 599 / 637
θ range for data	1.718 to 26.999	1.795 to 25.000
diffraction limits (*h*, *k*, *l*)	-28≤*h*≤28, -33≤*k*≤33,-20≤*l*≤20	-12≤*h*≤12, -18≤*k*≤18,-20≤*l*≤20
refinement method	Full-matrix least-squares on F^2	
R_1, wR_2 [$I>2\sigma(I)$]	R_1 = 0.0515[a], wR_2 = 0.1618[b]	R_1 = 0.0723[a], wR_2 = 0.1769[b]
R_1, wR_2 (all data)	R_1 = 0.0649[a], wR_2 = 0.1676[b]	R_1 = 0.1338[a], wR_2 = 0.2083[b]
largest peak, hole, eÅ^{-3}	0.670, -0.607	0.631, -0.666

[a] $R = \Sigma||F_o| - |F_c||/\Sigma|F_o|$. [b] $wR(F^2) = [\Sigma w(F_o^2 - F_c^2)^2/\Sigma w(F_o^2)^2]^{1/2}$ where $w = 1/[\sigma^2(F_o^2) + (0.0956P)^2 + (0.0000)P]$ for ***as-flex*MOF(CN)**, and $w = 1/[\sigma^2(F_o^2) + (0.1179P)^2 + (0.0000)P]$ for ***cp-flex*MOF(CN)**, $P = (F_o^2 + 2F_c^2)/3$.

Table S2. Selected bond distances [Å] and angles [°] of ***as-flex*MOF(CN)**.

Ni(1)-N(1)$^{\#1}$	2.0507(18)	Ni(2)-N(5)$^{\#2}$	2.0550(19)
Ni(1)-N(1)	2.0507(18)	Ni(2)-N(5)	2.0550(19)
Ni(1)-N(3)$^{\#1}$	2.0644(19)	Ni(2)-N(7)	2.056(2)
Ni(1)-N(3)	2.0645(19)	Ni(2)-N(7)$^{\#2}$	2.056(2)
Ni(1)-O(1)$^{\#1}$	2.1143(13)	Ni(2)-O(3)	2.1148(14)
Ni(1)-O(1)	2.1143(13)	Ni(2)-O(3)$^{\#2}$	2.1148(14)
N(1)$^{\#1}$-Ni(1)-N(1)	180.0	N(5)-Ni(2)-O(3)	92.71(7)
N(1)$^{\#1}$-Ni(1)-N(3)$^{\#1}$	94.21(8)	N(7)-Ni(2)-O(3)	90.53(7)
N(1)-Ni(1)-N(3)$^{\#1}$	85.79(8)	N(7)$^{\#2}$-Ni(2)-O(3)	89.47(7)
N(1)$^{\#1}$-Ni(1)-N(3)	85.79(8)	N(5)$^{\#2}$-Ni(2)-O(3)$^{\#2}$	92.71(7)
N(1)-Ni(1)-N(3)	94.21(8)	N(5)-Ni(2)-O(3)$^{\#2}$	87.29(7)
N(3)$^{\#1}$-Ni(1)-N(3)	180.0	N(7)-Ni(2)-O(3)$^{\#2}$	89.47(7)
N(1)$^{\#1}$-Ni(1)-O(1)$^{\#1}$	92.47(6)	N(7)$^{\#2}$-Ni(2)-O(3)$^{\#2}$	90.53(7)
N(1)-Ni(1)-O(1)$^{\#1}$	87.52(6)	O(3)-Ni(2)-O(3)$^{\#2}$	180.0
N(3)$^{\#1}$-Ni(1)-O(1)$^{\#1}$	86.50(7)	C(15)-O(1)-Ni(1)	135.76(13)
N(3)-Ni(1)-O(1)$^{\#1}$	93.50(7)	C(22)-O(3)-Ni(2)	133.11(15)
N(1)$^{\#1}$-Ni(1)-O(1)	87.53(6)	C(1)-N(1)-Ni(1)	105.72(14)
N(1)-Ni(1)-O(1)	92.47(6)	C(2)-N(1)-Ni(1)	112.64(13)
N(3)$^{\#1}$-Ni(1)-O(1)	93.50(7)	Ni(1)-N(1)-H(1)	108.3
N(3)-Ni(1)-O(1)	86.51(7)	C(4)-N(3)-Ni(1)	106.36(14)
O(1)$^{\#1}$-Ni(1)-O(1)	180.0	C(3)-N(3)-Ni(1)	113.62(15)
N(5)$^{\#2}$-Ni(2)-N(5)	180.0	Ni(1)-N(3)-H(3)	107.4
N(5)$^{\#2}$-Ni(2)-N(7)	85.27(9)	C(8)-N(5)-Ni(2)	106.52(17)
N(5)-Ni(2)-N(7)	94.73(9)	C(9)-N(5)-Ni(2)	114.92(16)
N(5)$^{\#2}$-Ni(2)-N(7)$^{\#2}$	94.73(9)	Ni(2)-N(5)-H(5)	106.6
N(5)-Ni(2)-N(7)$^{\#2}$	85.27(9)	C(11)-N(7)-Ni(2)	105.52(17)
N(7)-Ni(2)-N(7)$^{\#2}$	180.0	C(10)-N(7)-Ni(2)	113.08(16)
N(5)$^{\#2}$-Ni(2)-O(3)	87.29(7)	Ni(2)-N(7)-H(7)	108.0

Symmetry transformations used to generate equivalent atoms:
#1 –x+1, -y+1,-z #2 -x+3/2,-y+1/2,-z+1 #3 -x+1,y,-z+1/2

Table S3. Selected bond distances [Å] and angles [°] of ***cp-flex*MOF(CN)**.

Ni(1)-N(1)	2.043(4)	Ni(3)-N(10)	2.045(5)
Ni(1)-N(1)$^{\#1}$	2.043(4)	Ni(3)-N(10)$^{\#3}$	2.045(5)
Ni(1)-N(2)	2.043(5)	Ni(3)-N(9)	2.055(5)
Ni(1)-N(2)$^{\#1}$	2.043(5)	Ni(3)-N(9)$^{\#3}$	2.055(5)
Ni(1)-O(2)$^{\#1}$	2.180(4)	Ni(3)-O(6)$^{\#3}$	2.152(4)
Ni(1)-O(2)	2.180(4)	Ni(3)-O(6)	2.152(4)
Ni(2)-N(6)$^{\#2}$	2.055(5)	Ni(4)-N(13)	2.019(5)
Ni(2)-N(6)	2.055(5)	Ni(4)-N(13)$^{\#4}$	2.019(5)
Ni(2)-N(5)	2.072(6)	Ni(4)-N(14)	2.062(6)
Ni(2)-N(5)$^{\#2}$	2.072(6)	Ni(4)-N(14)$^{\#4}$	2.062(6)
Ni(2)-O(4)	2.129(4)	Ni(4)-O(8)	2.201(4)
Ni(2)-O(4)$^{\#2}$	2.129(4)	Ni(4)-O(8)$^{\#4}$	2.201(4)
N(1)-Ni(1)-N(1)$^{\#1}$	180.0	O(6)$^{\#3}$-Ni(3)-O(6)	180.0
N(1)-Ni(1)-N(2)	91.74(19)	N(13)-Ni(4)-N(13)$^{\#4}$	180.0
N(1)$^{\#1}$-Ni(1)-N(2)	88.26(19)	N(13)-Ni(4)-N(14)	94.9(2)
N(1)-Ni(1)-N(2)$^{\#1}$	88.26(19)	N(13)$^{\#4}$-Ni(4)-N(14)	85.1(2)
N(1)$^{\#1}$-Ni(1)-N(2)$^{\#1}$	91.74(19)	N(13)-Ni(4)-N(14)$^{\#4}$	85.1(2)
N(2)-Ni(1)-N(2)$^{\#1}$	180.0	N(13)$^{\#4}$-Ni(4)-N(14)$^{\#4}$	94.9(2)
N(1)-Ni(1)-O(2)$^{\#1}$	91.65(16)	N(14)-Ni(4)-N(14)$^{\#4}$	180.00(16)
N(1)$^{\#1}$-Ni(1)-O(2)$^{\#1}$	88.35(16)	N(13)-Ni(4)-O(8)	86.72(18)
N(2)-Ni(1)-O(2)$^{\#1}$	89.99(17)	N(13)$^{\#4}$-Ni(4)-O(8)	93.28(18)
N(2)$^{\#1}$-Ni(1)-O(2)$^{\#1}$	90.01(17)	N(14)-Ni(4)-O(8)	93.32(19)
N(1)-Ni(1)-O(2)	88.35(16)	N(14)$^{\#4}$-Ni(4)-O(8)	86.68(19)
N(1)$^{\#1}$-Ni(1)-O(2)	91.65(16)	N(13)-Ni(4)-O(8)$^{\#4}$	93.28(18)
N(2)-Ni(1)-O(2)	90.01(17)	N(13)$^{\#4}$-Ni(4)-O(8)$^{\#4}$	86.72(18)
N(2)$^{\#1}$-Ni(1)-O(2)	89.99(17)	N(14)-Ni(4)-O(8)$^{\#4}$	86.68(19)
O(2)$^{\#1}$-Ni(1)-O(2)	180.0	N(14)$^{\#4}$-Ni(4)-O(8)$^{\#4}$	93.32(19)
N(6)$^{\#2}$-Ni(2)-N(6)	180.0	O(8)-Ni(4)-O(8)$^{\#4}$	180.0
N(6)$^{\#2}$-Ni(2)-N(5)	86.1(3)	C(1)-O(2)-Ni(1)	131.2(4)
N(6)-Ni(2)-N(5)	93.9(3)	C(8)-O(4)-Ni(2)	136.9(4)
N(6)$^{\#2}$-Ni(2)-N(5)$^{\#2}$	93.9(3)	C(9)-O(6)-Ni(3)	131.9(4)
N(6)-Ni(2)-N(5)$^{\#2}$	86.1(3)	C(16)-O(8)-Ni(4)	129.9(4)
N(5)-Ni(2)-N(5)$^{\#2}$	180.0(3)	C(18)-N(1)-Ni(1)	119.0(3)
N(6)$^{\#2}$-Ni(2)-O(4)	87.61(19)	C(19)-N(1)-Ni(1)	103.4(4)
N(6)-Ni(2)-O(4)	92.39(19)	C(20)-N(2)-Ni(1)	103.2(4)

N(5)-Ni(2)-O(4)	86.4(2)	C(17)-N(2)-Ni(1)	113.7(4)
N(5)$^{\#2}$-Ni(2)-O(4)	93.6(2)	Ni(1)-N(2)-H(2)	108.4
N(6)$^{\#2}$-Ni(2)-O(4)$^{\#2}$	92.39(19)	C(27)-N(5)-Ni(2)	113.3(5)
N(6)-Ni(2)-O(4)$^{\#2}$	87.61(19)	C(25)-N(5)-Ni(2)	104.3(5)
N(5)-Ni(2)-O(4)$^{\#2}$	93.6(2)	Ni(2)-N(5)-H(5)	107.5
N(5)$^{\#2}$-Ni(2)-O(4)$^{\#2}$	86.4(2)	C(24)-N(6)-Ni(2)	105.9(5)
O(4)-Ni(2)-O(4)$^{\#2}$	180.0	C(26)-N(6)-Ni(2)	112.6(5)
N(10)-Ni(3)-N(10)$^{\#3}$	180.0	Ni(2)-N(6)-H(6)	108.5
N(10)-Ni(3)-N(9)	94.3(2)	C(34)-N(9)-Ni(3)	111.7(4)
N(10)$^{\#3}$-Ni(3)-N(9)	85.7(2)	C(32)-N(9)-Ni(3)	105.7(4)
N(10)-Ni(3)-N(9)$^{\#3}$	85.7(2)	C(33)-N(10)-Ni(3)	114.6(4)
N(10)$^{\#3}$-Ni(3)-N(9)$^{\#3}$	94.3(2)	C(31)-N(10)-Ni(3)	105.6(4)
N(9)-Ni(3)-N(9)$^{\#3}$	180.0	C(41)-N(13)-Ni(4)	113.6(4)
N(10)-Ni(3)-O(6)$^{\#3}$	88.66(19)	C(39)-N(13)-Ni(4)	107.8(4)
N(10)$^{\#3}$-Ni(3)-O(6)$^{\#3}$	91.34(19)	C(38)-N(14)-Ni(4)	106.5(4)
N(9)-Ni(3)-O(6)$^{\#3}$	91.49(19)	C(40)-N(14)-Ni(4)	113.0(4)
N(9)$^{\#3}$-Ni(3)-O(6)$^{\#3}$	88.51(19)	Ni(4)-N(14)-H(14)	108.3
N(9)$^{\#3}$-Ni(3)-O(6)	91.49(19)		

Symmetry transformations used to generate equivalent atoms:
#1 –x,-y+1,-z #2 -x,-y,-z+1 #3 –x+1,-y,-z #4 -x,-y+1,-z+1

Table S4. X-ray crystallographic data of ***as-flex*MOF(OH)** and ***cp-flex*MOF(OH)**.

Compound	***as-flex*MOF(OH)**	***cp-flex*MOF(OH)**
formula	$Ni_4C_{86}H_{146}N_{26}O_{26}$	$Ni_4C_{80}H_{132}N_{24}O_{24}$
crystal system	*Triclinic*	*Triclinic*
space group	*P*-1	*P*-1
fw	2195.12	2048.93
a, Å	15.210(3)	9.819(3)
b, Å	15.650(3)	15.316(3)
c, Å	17.099(3)	16.301(3)
α, deg	82.34(3)	90.994(10)
β, deg	65.07(3)	103.450(7)
γ, deg	75.54(3)	90.421(10)
V, Å^3	3572.3(16)	2383.7(10)
Z	1	1
ρ_{calcd}, g cm^{-3}	1.020	1.427
temp , K	220(2)	100(2)
λ, Å	0.700	0.700
μ, mm^{-1}	0.555	0.824
goodness-of-fit (F^2)	0.908	1.002
F(000)	1164	1084
reflections collected	28016	15154
independent reflections	14507 [*R*(int) = 0.0334]	8088 [*R*(int) = 0.0325]
completeness to θ_{max}, %	96.3%	92.0%
data/restraints/parameters	14057 / 648 / 676	8088 / 0 / 605
θ range for data	1.294 to 26.000	1.803 to 24.999
diffraction limits (*h*, *k*, *l*)	-19≤*h*≤19, -18≤*k*≤18,-21≤*l*≤21	-11≤*h*≤11, -18≤*k*≤18,-19≤*l*≤19
refinement method	Full-matrix least-squares on F^2	
R_1, wR_2 [$I>2\sigma(I)$]	$R_1 = 0.0711^a$, $wR_2 = 0.2121^b$	$R_1 = 0.0837^a$, $wR_2 = 0.2282^b$
R_1, wR_2 (all data)	$R_1 = 0.1240^a$, $wR_2 = 0.2303^b$	$R_1 = 0.1226^a$, $wR_2 = 0.2616^b$
largest peak, hole, eÅ^{-3}	0.789, -0.545	0.918, -0.722

$^aR = \Sigma||F_o| - |F_c||/\Sigma|F_o|$. $^bwR(F^2) = [\Sigma w(F_o^2 - F_c^2)^2/\Sigma w(F_o^2)^2]^{1/2}$ where $w = 1/[\sigma^2(F_o^2) + (0.1367P)^2 + (0.0000)P]$ for ***as-flex*MOF(OH)**, and $w = 1/[\sigma^2(F_o^2) + (0.1810P)^2 + (0.0000)P]$ for ***cp-flex*MOF(OH)**, $P = (F_o^2 + 2F_c^2)/3$.

Table S5. Selected bond distances [Å] and angles [°] of ***as-flex*MOF(OH)**.

Ni(1)-N(3)	2.043(4)	Ni(2)-N(4)$^{\#2}$	2.062(4)
Ni(1)-N(3)$^{\#1}$	2.043(4)	Ni(2)-O(7)	2.115(3)
Ni(1)-N(1)	2.066(4)	Ni(2)-O(7)$^{\#2}$	2.115(3)
Ni(1)-N(1)$^{\#1}$	2.066(4)	Ni(3)-N(9)	2.055(5)
Ni(1)-O(5)	2.159(3)	Ni(3)-N(9)$^{\#3}$	2.055(5)
Ni(1)-O(5)$^{\#1}$	2.159(3)	Ni(3)-N(7)	2.067(4)
Ni(2)-N(6)$^{\#2}$	2.060(4)	Ni(3)-N(7)$^{\#3}$	2.067(4)
Ni(2)-N(6)	2.060(4)	Ni(3)-O(9)$^{\#3}$	2.129(3)
Ni(2)-N(4)	2.062(4)	Ni(3)-O(9)	2.129(3)
N(3)-Ni(1)-N(3)$^{\#1}$	180.0	N(9)-Ni(3)-N(7)	94.31(18)
N(3)-Ni(1)-N(1)	93.77(16)	N(9)$^{\#3}$-Ni(3)-N(7)	85.69(18)
N(3)$^{\#1}$-Ni(1)-N(1)	86.23(16)	N(9)-Ni(3)-N(7)$^{\#3}$	85.69(18)
N(3)-Ni(1)-N(1)$^{\#1}$	86.23(16)	N(9)$^{\#3}$-Ni(3)-N(7)$^{\#3}$	94.31(18)
N(3)$^{\#1}$-Ni(1)-N(1)$^{\#1}$	93.77(16)	N(7)-Ni(3)-N(7)$^{\#3}$	180.0
N(1)-Ni(1)-N(1)$^{\#1}$	180.0	N(9)-Ni(3)-O(9)$^{\#3}$	93.66(16)
N(3)-Ni(1)-O(5)	87.51(14)	N(9)$^{\#3}$-Ni(3)-O(9)$^{\#3}$	86.34(15)
N(3)$^{\#1}$-Ni(1)-O(5)	92.49(15)	N(7)-Ni(3)-O(9)$^{\#3}$	88.32(14)
N(1)-Ni(1)-O(5)	92.74(14)	N(7)$^{\#3}$-Ni(3)-O(9)$^{\#3}$	91.68(14)
N(1)$^{\#1}$-Ni(1)-O(5)	87.26(14)	N(9)-Ni(3)-O(9)	86.34(15)
N(3)-Ni(1)-O(5)$^{\#1}$	92.49(15)	N(9)$^{\#3}$-Ni(3)-O(9)	93.66(15)
N(3)$^{\#1}$-Ni(1)-O(5)$^{\#1}$	87.51(15)	N(7)-Ni(3)-O(9)	91.68(14)
N(1)-Ni(1)-O(5)$^{\#1}$	87.26(14)	N(7)$^{\#3}$-Ni(3)-O(9)	88.32(14)
N(1)$^{\#1}$-Ni(1)-O(5)$^{\#1}$	92.74(14)	O(9)$^{\#3}$-Ni(3)-O(9)	180.0
O(5)-Ni(1)-O(5)$^{\#1}$	180.0	C(14)-N(7)-Ni(3)	113.3(4)
C(1)-N(1)-Ni(1)	104.9(3)	C(13)-N(7)-Ni(3)	105.3(3)
C(2)-N(1)-Ni(1)	113.7(3)	C(15)-N(9)-Ni(3)	114.0(4)
Ni(1)-N(1)-H(1)	108.1	C(16)-N(9)-Ni(3)	106.5(3)
C(4)-N(3)-Ni(1)	107.6(3)	Ni(3)-N(9)-H(9)	107.3
C(3)-N(3)-Ni(1)	115.4(3)	N(10)$^{\#4}$-Ni(4)-N(10)	180.0
Ni(1)-N(3)-H(3)	107.5	N(10)$^{\#4}$-Ni(4)-N(12)$^{\#4}$	94.9(2)
N(6)$^{\#2}$-Ni(2)-N(6)	180.0	N(10)-Ni(4)-N(12)$^{\#4}$	85.1(2)
N(6)$^{\#2}$-Ni(2)-N(4)	85.28(17)	N(10)$^{\#4}$-Ni(4)-N(12)	85.1(2)
N(6)-Ni(2)-N(4)	94.72(17)	N(10)-Ni(4)-N(12)	94.9(2)
N(6)$^{\#2}$-Ni(2)-N(4)$^{\#2}$	94.72(17)	N(12)$^{\#4}$-Ni(4)-N(12)	180.0
N(6)-Ni(2)-N(4)$^{\#2}$	85.29(17)	N(10)$^{\#4}$-Ni(4)-O(11)	87.68(16)

N(4)-Ni(2)-N(4)$^{\#2}$	180.0	N(10)-Ni(4)-O(11)	92.32(16)
N(6)$^{\#2}$-Ni(2)-O(7)	92.76(14)	N(12)$^{\#4}$-Ni(4)-O(11)	93.64(15)
N(6)-Ni(2)-O(7)	87.24(14)	N(12)-Ni(4)-O(11)	86.36(15)
N(4)-Ni(2)-O(7)	90.91(14)	N(10)$^{\#4}$-Ni(4)-O(11)$^{\#4}$	92.32(16)
N(4)$^{\#2}$-Ni(2)-O(7)	89.09(14)	N(10)-Ni(4)-O(11)$^{\#4}$	87.68(16)
N(6)$^{\#2}$-Ni(2)-O(7)$^{\#2}$	87.24(14)	N(12)$^{\#4}$-Ni(4)-O(11)$^{\#4}$	86.35(15)
N(6)-Ni(2)-O(7)$^{\#2}$	92.76(14)	N(12)-Ni(4)-O(11)$^{\#4}$	93.65(15)
N(4)-Ni(2)-O(7)$^{\#2}$	89.09(14)	O(11)-Ni(4)-O(11)$^{\#4}$	180.0
N(4)$^{\#2}$-Ni(2)-O(7)$^{\#2}$	90.91(14)	C(19)-N(10)-Ni(4)	105.3(4)
O(7)-Ni(2)-O(7)$^{\#2}$	180.0	C(20)-N(10)-Ni(4)	113.0(4)
C(7)-N(4)-Ni(2)	107.0(3)	Ni(4)-N(10)-H(10)	107.6
C(8)-N(4)-Ni(2)	113.2(3)	C(22)-N(12)-Ni(4)	107.5(4)
Ni(2)-N(4)-H(4)	107.4	C(21)-N(12)-Ni(4)	114.4(4)
C(9)-N(6)-Ni(2)	113.5(3)	Ni(4)-N(12)-H(12)	106.9
C(10)-N(6)-Ni(2)	105.8(3)	C(25)-O(5)-Ni(1)	134.7(3)
Ni(2)-N(6)-H(6)	107.8	C(32)-O(7)-Ni(2)	138.9(3)
N(4)-C(7)-C(10)$^{\#2}$	108.2(4)	C(33)-O(9)-Ni(3)	135.8(3)
N(9)-Ni(3)-N(9)$^{\#3}$	180.0	C(40)-O(11)-Ni(4)	133.4(3)

Symmetry transformations used to generate equivalent atoms:
#1 –x+1,-y+2,-z #2 -x+1,-y+1,-z+1 #3 -x+1,-y+1,-z #4 -x,-y+2,-z+1

Table S6. Selected bond distances [Å] and angles [°] of ***cp-flex*MOF(OH)**.

Ni(1)-N(1)	2.045(5)	Ni(3)-N(7)	2.047(5)
Ni(1)-N(1)$^{\#1}$	2.045(5)	Ni(3)-N(7)$^{\#3}$	2.047(5)
Ni(1)-N(2)	2.045(5)	Ni(3)-N(8)$^{\#3}$	2.053(6)
Ni(1)-N(2)$^{\#1}$	2.045(5)	Ni(3)-N(8)	2.053(6)
Ni(1)-O(2)$^{\#1}$	2.126(4)	Ni(3)-O(6)$^{\#3}$	2.162(4)
Ni(1)-O(2)	2.126(4)	Ni(3)-O(6)	2.162(4)
Ni(2)-N(5)$^{\#2}$	2.023(5)	Ni(4)-N(10)$^{\#4}$	2.028(6)
Ni(2)-N(5)	2.023(5)	Ni(4)-N(10)	2.028(6)
Ni(2)-N(4)	2.041(6)	Ni(4)-N(11)	2.061(6)
Ni(2)-N(4)$^{\#2}$	2.041(6)	Ni(4)-N(11)$^{\#4}$	2.061(6)
Ni(2)-O(4)	2.167(4)	Ni(4)-O(8)	2.143(4)
Ni(2)-O(4)$^{\#2}$	2.167(4)	Ni(4)-O(8)$^{\#4}$	2.143(4)
N(1)-Ni(1)-N(1)$^{\#1}$	180.0	N(8)-Ni(3)-O(6)	88.52(19)
N(1)-Ni(1)-N(2)	92.7(2)	O(6)$^{\#3}$-Ni(3)-O(6)	180.0
N(1)$^{\#1}$-Ni(1)-N(2)	87.3(2)	N(10)$^{\#4}$-Ni(4)-N(10)	180.0(2)
N(1)-Ni(1)-N(2)$^{\#1}$	87.3(2)	N(10)$^{\#4}$-Ni(4)-N(11)	86.0(2)
N(1)$^{\#1}$-Ni(1)-N(2)$^{\#1}$	92.7(2)	N(10)-Ni(4)-N(11)	94.0(2)
N(2)-Ni(1)-N(2)$^{\#1}$	180.0(3)	N(10)$^{\#4}$-Ni(4)-N(11)$^{\#4}$	94.0(2)
N(1)-Ni(1)-O(2)$^{\#1}$	93.78(19)	N(10)-Ni(4)-N(11)$^{\#4}$	86.0(2)
N(1)$^{\#1}$-Ni(1)-O(2)$^{\#1}$	86.22(19)	N(11)-Ni(4)-N(11)$^{\#4}$	180.00(3)
N(2)-Ni(1)-O(2)$^{\#1}$	87.49(18)	N(10)$^{\#4}$-Ni(4)-O(8)	92.11(19)
N(2)$^{\#1}$-Ni(1)-O(2)$^{\#1}$	92.51(18)	N(10)-Ni(4)-O(8)	87.89(19)
N(1)-Ni(1)-O(2)	86.22(19)	N(11)-Ni(4)-O(8)	92.31(19)
N(1)$^{\#1}$-Ni(1)-O(2)	93.78(19)	N(11)$^{\#4}$-Ni(4)-O(8)	87.69(19)
N(2)-Ni(1)-O(2)	92.51(18)	N(10)$^{\#4}$-Ni(4)-O(8)$^{\#4}$	87.89(19)
N(2)$^{\#1}$-Ni(1)-O(2)	87.49(18)	N(10)-Ni(4)-O(8)$^{\#4}$	92.11(19)
O(2)$^{\#1}$-Ni(1)-O(2)	180.0	N(11)-Ni(4)-O(8)$^{\#4}$	87.69(19)
N(5)$^{\#2}$-Ni(2)-N(5)	180.0	N(11)$^{\#4}$-Ni(4)-O(8)$^{\#4}$	92.31(19)
N(5)$^{\#2}$-Ni(2)-N(4)	85.6(2)	O(8)-Ni(4)-O(8)$^{\#4}$	180.0(3)
N(5)-Ni(2)-N(4)	94.4(2)	C(1)-O(2)-Ni(1)	137.5(4)
N(5)$^{\#2}$-Ni(2)-N(4)$^{\#2}$	94.4(2)	C(9)-O(4)-Ni(2)	131.2(4)
N(5)-Ni(2)-N(4)$^{\#2}$	85.6(2)	C(16)-O(6)-Ni(3)	131.1(4)
N(4)-Ni(2)-N(4)$^{\#2}$	180.0	C(8)-O(8)-Ni(4)	133.0(4)
N(5)$^{\#2}$-Ni(2)-O(4)	87.94(18)	C(20)-N(1)-Ni(1)	115.1(4)
N(5)-Ni(2)-O(4)	92.06(18)	C(18)-N(1)-Ni(1)	104.9(4)

N(4)-Ni(2)-O(4)	87.4(2)	C(19)-N(2)-Ni(1)	114.4(4)
N(4)$^{\#2}$-Ni(2)-O(4)	92.6(2)	C(17)-N(2)-Ni(1)	104.6(4)
N(5)$^{\#2}$-Ni(2)-O(4)$^{\#2}$	92.06(18)	Ni(1)-N(2)-H(2)	108.2
N(5)-Ni(2)-O(4)$^{\#2}$	87.94(18)	C(23)-N(4)-Ni(2)	106.4(5)
N(4)-Ni(2)-O(4)$^{\#2}$	92.6(2)	C(26)-N(4)-Ni(2)	113.4(4)
N(4)$^{\#2}$-Ni(2)-O(4)$^{\#2}$	87.4(2)	Ni(2)-N(4)-H(4)	107.3
O(4)-Ni(2)-O(4)$^{\#2}$	180.0(2)	C(24)-N(5)-Ni(2)	106.3(4)
N(7)-Ni(3)-N(7)$^{\#3}$	180.0	C(25)-N(5)-Ni(2)	115.0(4)
N(7)-Ni(3)-N(8)$^{\#3}$	85.6(2)	C(29)-N(7)-Ni(3)	107.3(4)
N(7)$^{\#3}$-Ni(3)-N(8)$^{\#3}$	94.4(2)	C(31)-N(7)-Ni(3)	113.4(4)
N(7)-Ni(3)-N(8)	94.4(2)	C(30)-N(8)-Ni(3)	105.4(4)
N(7)$^{\#3}$-Ni(3)-N(8)	85.6(2)	C(32)-N(8)-Ni(3)	112.8(4)
N(8)$^{\#3}$-Ni(3)-N(8)	180.0	Ni(3)-N(8)-H(8)	108.2
N(7)-Ni(3)-O(6)$^{\#3}$	86.26(18)	C(35)-N(10)-Ni(4)	105.6(4)
N(7)$^{\#3}$-Ni(3)-O(6)$^{\#3}$	93.74(18)	C(37)-N(10)-Ni(4)	114.4(4)
N(8)$^{\#3}$-Ni(3)-O(6)$^{\#3}$	88.52(19)	Ni(4)-N(10)-H(10)	107.3
N(8)-Ni(3)-O(6)$^{\#3}$	91.48(19)	C(38)-N(11)-Ni(4)	114.8(5)
N(7)-Ni(3)-O(6)	93.74(18)	C(36)-N(11)-Ni(4)	104.9(4)
N(7)$^{\#3}$-Ni(3)-O(6)	86.26(18)	Ni(4)-N(11)-H(11A)	106.8
N(8)$^{\#3}$-Ni(3)-O(6)	91.48(19)		

Symmetry transformations used to generate equivalent atoms:
#1 –x+1,-y+2,-z #2 -x+2,-y+2,-z+1 #3 -x+1,-y+1,-z #4 -x+1,-y+1,-z+1

Table S7. X-ray crystallographic data of ***as-flex*MOF(CH$_2$)** and ***cp-flex*MOF(CH$_2$)**.

Compound	***as-flex*MOF(CH$_2$)**	***cp-flex*MOF(CH$_2$)**
formula	$Ni_2C_{48}H_{72}N_{14}O_8$	$Ni_4C_{88}H_{132}N_{24}O_{16}$
crystal system	*Monoclinic*	*Triclinic*
space group	*C*2/*c*	*P*-1
fw	1090.61	2017.01
a, Å	12.920(3)	9.829(3)
b, Å	32.634(6)	14.867(3)
c, Å	15.617(3)	16.595(4)
α, deg	90	90.112(7)
β, deg	105.16(3)	78.434(10)
γ, deg	90	87.888(10)
V, Å^3	6355(2)	2374.0(10)
Z	4	1
ρ_{calcd}, g cm^{-3}	1.140	1.411
temp , K	220(2)	100(2)
λ, Å	0.610	0.700
μ, mm^{-1}	0.428	0.821
goodness-of-fit (F^2)	1.127	1.001
F(000)	2312	1068
reflections collected	31733	15074
independent reflections	8742 [*R*(int) = 0.0434]	8042 [*R*(int) = 0.0671]
completeness to θ_{max}, %	98.9%	92.1%
data/restraints/parameters	8742 / 296 / 321	8042 / 546 / 601
θ range for data	1.500 to 25.000	2.199 to 25.000
diffraction limits (*h*, *k*, *l*)	-17≤*h*≤17, -45≤*k*≤45,-21≤*l*≤21	-11≤*h*≤11, -17≤*k*≤17,-20≤*l*≤20
refinement method	Full-matrix least-squares on F^2	
R_1, wR_2 [$I>2\sigma(I)$]	$R_1 = 0.0784^a$, $wR_2 = 0.2657^b$	$R_1 = 0.0852^a$, $wR_2 = 0.2236^b$
R_1, wR_2 (all data)	$R_1 = 0.0873^a$, $wR_2 = 0.2778^b$	$R_1 = 0.1622^a$, $wR_2 = 0.2702^b$
largest peak, hole, eÅ^{-3}	1.270, -0.731	0.781, -0.487

$^aR = \Sigma||F_o| - |F_c||/\Sigma|F_o|$. $^bwR(F^2) = [\Sigma w(F_o^2 - F_c^2)^2/\Sigma w(F_o^2)^2]^{1/2}$ where $w = 1/[\sigma^2(F_o^2) + (0.1896P)^2 + (1.3860)P]$ for ***as-flex*MOF(CH$_2$)**, and $w = 1/[\sigma^2(F_o^2) + (0.1536P)^2 + (0.0000)P]$ for ***cp-flex*MOF(CH$_2$)**, $P = (F_o^2 + 2F_c^2)/3$.

Table S8. Selected bond distances [Å] and angles [°] of ***as-flex*MOF(CH$_2$)**.

Ni(1)-N(3)	2.059(2)	Ni(2)-N(4)$^{\#2}$	2.036(3)
Ni(1)-N(3)$^{\#1}$	2.059(2)	Ni(2)-N(4)	2.036(3)
Ni(1)-N(1)	2.063(3)	Ni(2)-N(6)	2.046(5)
Ni(1)-N(1)$^{\#1}$	2.063(3)	Ni(2)-N(6)$^{\#2}$	2.046(5)
Ni(1)-O(1)	2.1376(17)	Ni(2)-O(3)$^{\#2}$	2.1190(19)
Ni(1)-O(1)$^{\#1}$	2.1376(17)	Ni(2)-O(3)	2.1191(19)
N(3)-Ni(1)-N(3)$^{\#1}$	180.0	N(4)$^{\#2}$-Ni(2)-N(6)	88.6(2)
N(3)-Ni(1)-N(1)	93.88(10)	N(4)-Ni(2)-N(6)	91.4(2)
N(3)$^{\#1}$-Ni(1)-N(1)	86.12(10)	N(4)$^{\#2}$-Ni(2)-N(6)$^{\#2}$	91.4(2)
N(3)-Ni(1)-N(1)$^{\#1}$	86.13(10)	N(4)-Ni(2)-N(6)$^{\#2}$	88.6(2)
N(3)$^{\#1}$-Ni(1)-N(1)$^{\#1}$	93.87(10)	N(6)-Ni(2)-N(6)$^{\#2}$	180.0
N(1)-Ni(1)-N(1)$^{\#1}$	180.00(10)	N(4)$^{\#2}$-Ni(2)-O(3)$^{\#2}$	94.71(11)
N(3)-Ni(1)-O(1)	93.69(8)	N(4)-Ni(2)-O(3)$^{\#2}$	85.29(11)
N(3)$^{\#1}$-Ni(1)-O(1)	86.31(8)	N(6)-Ni(2)-O(3)$^{\#2}$	93.15(17)
N(1)-Ni(1)-O(1)	90.03(9)	N(6)$^{\#2}$-Ni(2)-O(3)$^{\#2}$	86.85(17)
N(1)$^{\#1}$-Ni(1)-O(1)	89.97(9)	N(4)$^{\#2}$-Ni(2)-O(3)	85.28(11)
N(3)-Ni(1)-O(1)$^{\#1}$	86.31(8)	N(4)-Ni(2)-O(3)	94.72(11)
N(3)$^{\#1}$-Ni(1)-O(1)$^{\#1}$	93.69(8)	N(6)-Ni(2)-O(3)	86.85(17)
N(1)-Ni(1)-O(1)$^{\#1}$	89.97(9)	N(6)$^{\#2}$-Ni(2)-O(3)	93.15(17)
N(1)$^{\#1}$-Ni(1)-O(1)$^{\#1}$	90.03(9)	O(3)$^{\#2}$-Ni(2)-O(3)	180.00(14)
O(1)-Ni(1)-O(1)$^{\#1}$	180.0	C(9)-N(4)-Ni(2)	120.9(4)
C(1)-N(1)-Ni(1)	104.8(2)	C(8)-N(4)-Ni(2)	103.0(3)
C(2)-N(1)-Ni(1)	113.39(19)	Ni(2)-N(4)-H(4)	107.9
Ni(1)-N(1)-H(1)	108.4	C(11)-N(6)-Ni(2)	111.8(5)
C(4)-N(3)-Ni(1)	105.96(18)	C(10)-N(6)-Ni(2)	116.4(4)
C(3)-N(3)-Ni(1)	114.12(17)	Ni(2)-N(6)-H(6A)	96.2
Ni(1)-N(3)-H(3)	107.5	C(15)-O(1)-Ni(1)	130.48(16)
N(4)$^{\#2}$-Ni(2)-N(4)	180.0	C(22)-O(3)-Ni(2)	131.20(19)

Symmetry transformations used to generate equivalent atoms:
#1 -x+3/2,-y+3/2,-z+1 #2 –x+1,-y+1,-z #3 –x+1,y,-z+1/2

Table S9. Selected bond distances [Å] and angles [°] of ***cp-flex*MOF(CH_2)**.

Ni(1)-N(2)$^{\#1}$	2.057(6)	Ni(3)-N(7)$^{\#3}$	2.043(7)
Ni(1)-N(2)	2.057(6)	Ni(3)-N(7)	2.043(7)
Ni(1)-N(1)	2.061(7)	Ni(3)-N(8)$^{\#3}$	2.060(8)
Ni(1)-N(1)$^{\#1}$	2.061(7)	Ni(3)-N(8)	2.060(8)
Ni(1)-O(2)$^{\#1}$	2.111(5)	Ni(3)-O(6)	2.171(5)
Ni(1)-O(2)	2.111(5)	Ni(3)-O(6)$^{\#3}$	2.171(5)
Ni(2)-N(5)	2.012(7)	Ni(4)-N(11)$^{\#4}$	2.027(7)
Ni(2)-N(5)$^{\#2}$	2.012(7)	Ni(4)-N(11)	2.027(7)
Ni(2)-N(4)$^{\#2}$	2.078(7)	Ni(4)-N(10)$^{\#4}$	2.058(9)
Ni(2)-N(4)	2.078(7)	Ni(4)-N(10)	2.058(9)
Ni(2)-O(4)$^{\#2}$	2.170(5)	Ni(4)-O(8)$^{\#4}$	2.135(6)
Ni(2)-O(4)	2.170(5)	Ni(4)-O(8)	2.135(6)
N(2)$^{\#1}$-Ni(1)-N(2)	180.0(4)	N(8)-Ni(3)-O(6)$^{\#3}$	91.2(2)
N(2)$^{\#1}$-Ni(1)-N(1)	84.1(3)	O(6)-Ni(3)-O(6)$^{\#3}$	180.0
N(2)-Ni(1)-N(1)	95.9(3)	N(11)$^{\#4}$-Ni(4)-N(11)	180.0
N(2)$^{\#1}$-Ni(1)-N(1)$^{\#1}$	95.9(3)	N(11)$^{\#4}$-Ni(4)-N(10)$^{\#4}$	92.5(4)
N(2)-Ni(1)-N(1)$^{\#1}$	84.1(3)	N(11)-Ni(4)-N(10)$^{\#4}$	87.5(4)
N(1)-Ni(1)-N(1)$^{\#1}$	180.0	N(11)$^{\#4}$-Ni(4)-N(10)	87.5(4)
N(2)$^{\#1}$-Ni(1)-O(2)$^{\#1}$	85.8(2)	N(11)-Ni(4)-N(10)	92.5(4)
N(2)-Ni(1)-O(2)$^{\#1}$	94.2(2)	N(10)$^{\#4}$-Ni(4)-N(10)	180.0
N(1)-Ni(1)-O(2)$^{\#1}$	87.9(2)	N(11)$^{\#4}$-Ni(4)-O(8)$^{\#4}$	94.8(3)
N(1)$^{\#1}$-Ni(1)-O(2)$^{\#1}$	92.1(2)	N(11)-Ni(4)-O(8)$^{\#4}$	85.2(3)
N(2)$^{\#1}$-Ni(1)-O(2)	94.2(2)	N(10)$^{\#4}$-Ni(4)-O(8)$^{\#4}$	87.7(3)
N(2)-Ni(1)-O(2)	85.8(2)	N(10)-Ni(4)-O(8)$^{\#4}$	92.3(3)
N(1)-Ni(1)-O(2)	92.1(2)	N(11)$^{\#4}$-Ni(4)-O(8)	85.2(3)
N(1)$^{\#1}$-Ni(1)-O(2)	87.9(2)	N(11)-Ni(4)-O(8)	94.8(3)
O(2)$^{\#1}$-Ni(1)-O(2)	180.0	N(10)$^{\#4}$-Ni(4)-O(8)	92.3(3)
N(5)-Ni(2)-N(5)$^{\#2}$	180.0	N(10)-Ni(4)-O(8)	87.7(3)
N(5)-Ni(2)-N(4)$^{\#2}$	85.6(3)	O(8)$^{\#4}$-Ni(4)-O(8)	180.0
N(5)$^{\#2}$-Ni(2)-N(4)$^{\#2}$	94.4(3)	C(1)-O(2)-Ni(1)	132.0(5)
N(5)-Ni(2)-N(4)	94.4(3)	C(16)-O(4)-Ni(2)	129.9(5)
N(5)$^{\#2}$-Ni(2)-N(4)	85.6(3)	C(9)-O(6)-Ni(3)	131.8(5)
N(4)$^{\#2}$-Ni(2)-N(4)	180.0	C(8)-O(8)-Ni(4)	133.9(5)
N(5)-Ni(2)-O(4)$^{\#2}$	87.1(2)	C(17)-N(1)-Ni(1)	106.0(5)
N(5)$^{\#2}$-Ni(2)-O(4)$^{\#2}$	92.9(2)	C(19)-N(1)-Ni(1)	113.2(5)

N(4)$^{\#2}$-Ni(2)-O(4)$^{\#2}$	85.7(2)	Ni(1)-N(1)-H(1)	107.5
N(4)-Ni(2)-O(4)$^{\#2}$	94.3(2)	C(18)-N(2)-Ni(1)	107.0(5)
N(5)-Ni(2)-O(4)	92.9(2)	C(20)-N(2)-Ni(1)	112.4(5)
N(5)$^{\#2}$-Ni(2)-O(4)	87.1(2)	Ni(1)-N(2)-H(2)	106.6
N(4)$^{\#2}$-Ni(2)-O(4)	94.3(2)	C(24)-N(4)-Ni(2)	104.2(5)
N(4)-Ni(2)-O(4)	85.7(2)	C(27)-N(4)-Ni(2)	112.5(5)
O(4)$^{\#2}$-Ni(2)-O(4)	180.0	Ni(2)-N(4)-H(4)	107.7
N(7)$^{\#3}$-Ni(3)-N(7)	180.0	C(26)-N(5)-Ni(2)	115.7(6)
N(7)$^{\#3}$-Ni(3)-N(8)$^{\#3}$	93.7(3)	C(25)-N(5)-Ni(2)	105.9(5)
N(7)-Ni(3)-N(8)$^{\#3}$	86.3(3)	C(31)-N(7)-Ni(3)	105.5(5)
N(7)$^{\#3}$-Ni(3)-N(8)	86.3(3)	C(33)-N(7)-Ni(3)	114.4(6)
N(7)-Ni(3)-N(8)	93.7(3)	Ni(3)-N(7)-H(7)	108.0
N(8)$^{\#3}$-Ni(3)-N(8)	180.0(4)	C(32)-N(8)-Ni(3)	105.1(6)
N(7)$^{\#3}$-Ni(3)-O(6)	87.2(2)	C(34)-N(8)-Ni(3)	113.8(6)
N(7)-Ni(3)-O(6)	92.8(2)	Ni(3)-N(8)-H(8)	108.0
N(8)$^{\#3}$-Ni(3)-O(6)	91.2(2)	C(38)-N(10)-Ni(4)	114.1(8)
N(8)-Ni(3)-O(6)	88.8(2)	C(40)-N(10)-Ni(4)	104.6(7)
N(7)$^{\#3}$-Ni(3)-O(6)$^{\#3}$	92.8(2)	Ni(4)-N(10)-H(10)	107.1
N(7)-Ni(3)-O(6)$^{\#3}$	87.2(2)	C(39)-N(11)-Ni(4)	117.0(7)
N(8)$^{\#3}$-Ni(3)-O(6)$^{\#3}$	88.8(2)	C(41)-N(11)-Ni(4)	104.4(6)

Symmetry transformations used to generate equivalent atoms:
#1 –x+1,-y+1,-z #2 –x+2,-y,-z #3 -x+1,-y+1,-z+1 #4 -x+1,-y,-z+1

Table S10. Lennard-Jones parameters and charge of adsorbate.

Adsorbate	ε/k_B **(K)**	σ **(Å)**	q
C_{CO_2}	27.0	2.80	0.70
O_{CO_2}	79.0	3.05	-0.35

Table S11. GCMC CO_2 adsorption simulation results at 196 K and 1 bar in ***as-flex*MOF(CN)** and ***as-flex*MOF(CH_2)**.

CO_2 Uptake	mmol/g	cm^3/g (STP)	cm^3 (STP)/cm^3
***as-flex*MOF(CN)**	13.9(1)	312(3)	258(3)
***as-flex*MOF(CH_2)**	5.4(3)	121(6)	132(6)

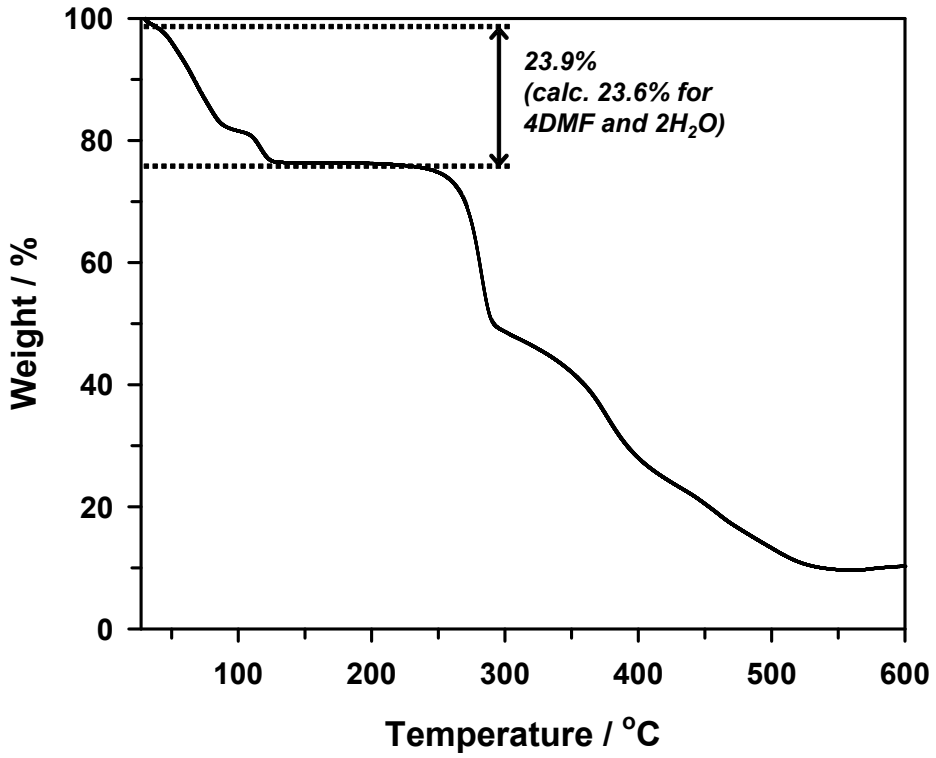

Figure S1. TGA trace of ***as-flex*MOF(CN)** obtained under a nitrogen atmosphere with 5 ^{o}C/min ramping rate.

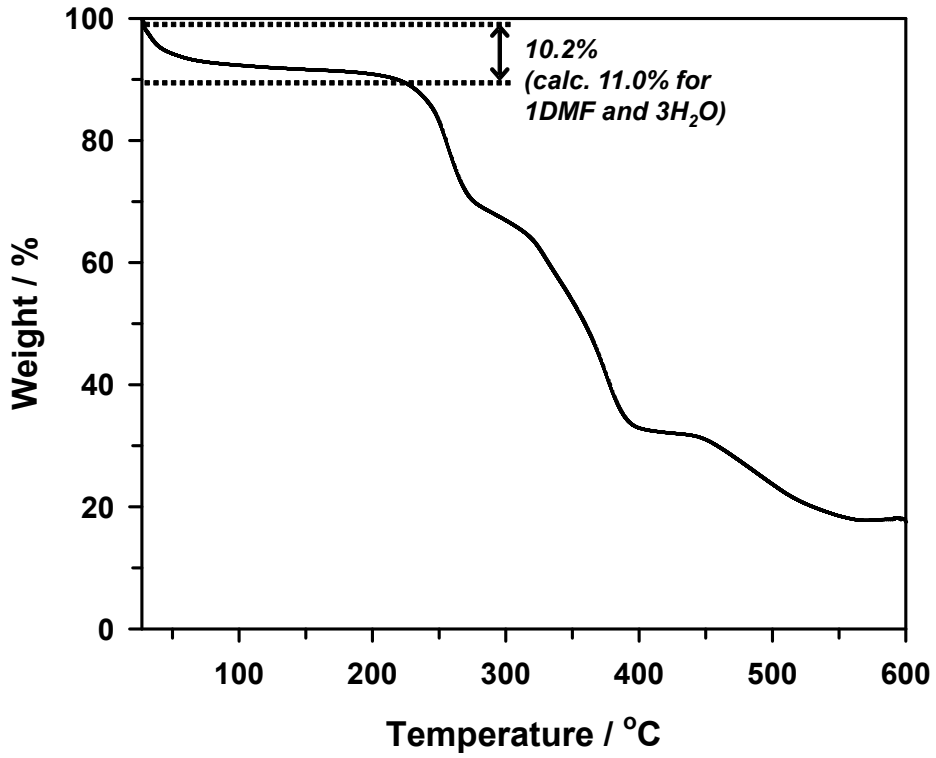

Figure S2. TGA trace of ***as-flex*MOF(OH)** obtained under a nitrogen atmosphere with 5 ^{o}C/min ramping rate.

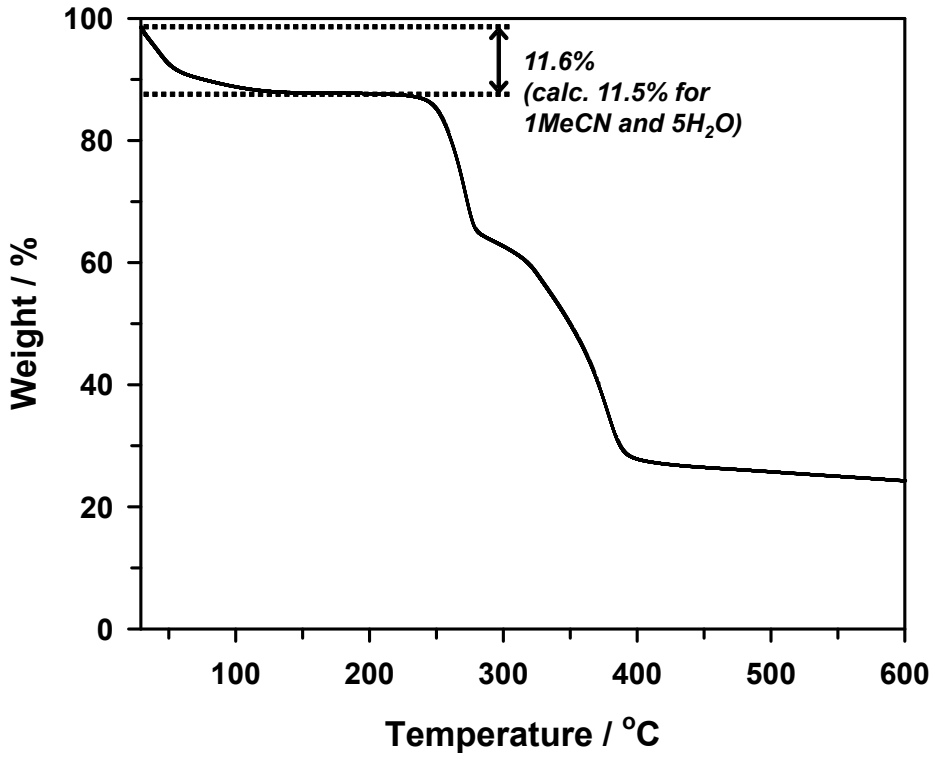

Figure S3. TGA trace of ***as-flex*MOF(CH_2)** obtained under a nitrogen atmosphere with 5 ^{o}C/min ramping rate.

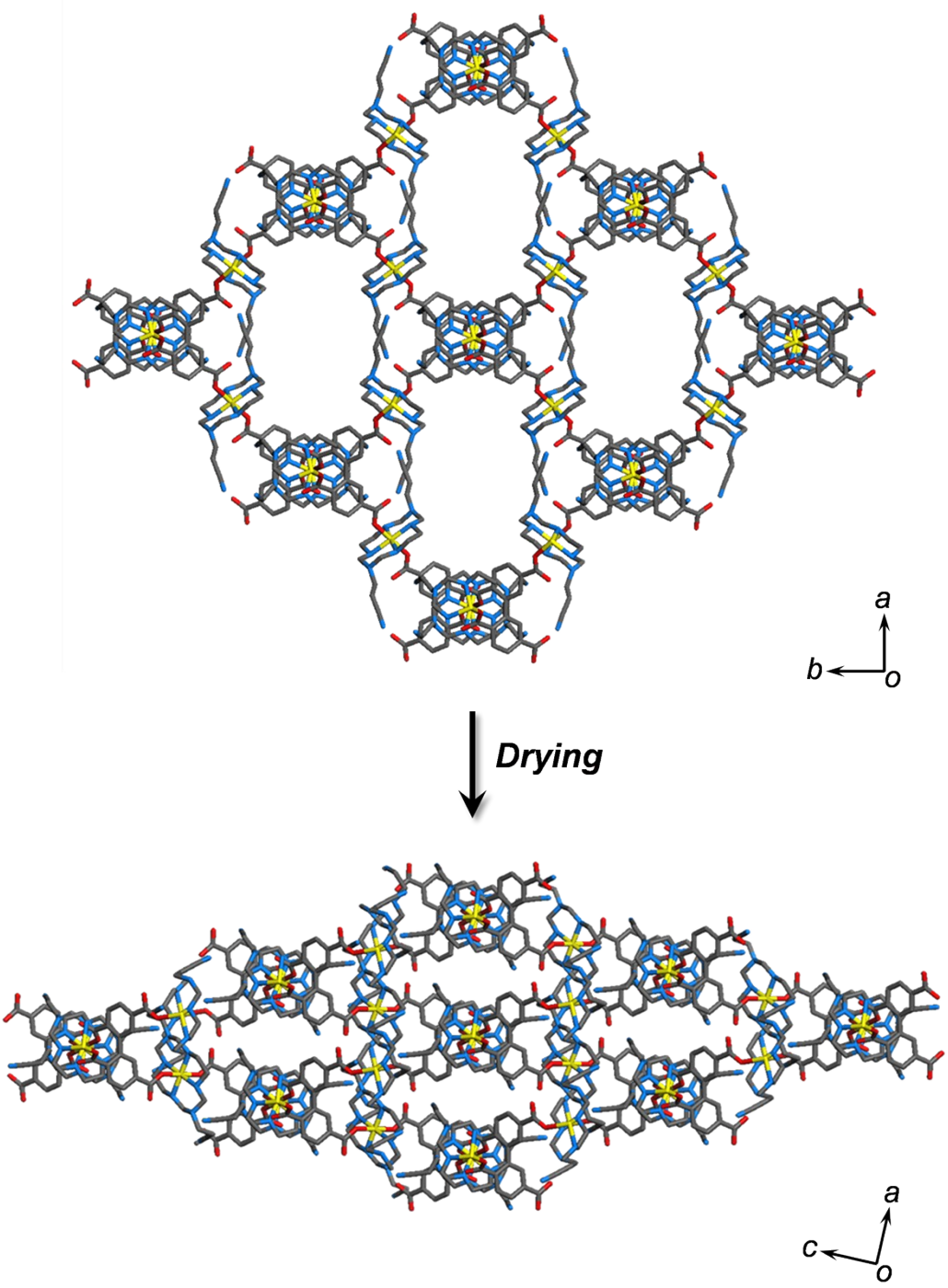

Figure S4. Comparison of SCD structures of ***as-flex*MOF(CN)** and ***cp-flex*MOF(CN)**, shown in the specific plane. Color scheme: Ni, yellow; C, black; O, red; N, blue.

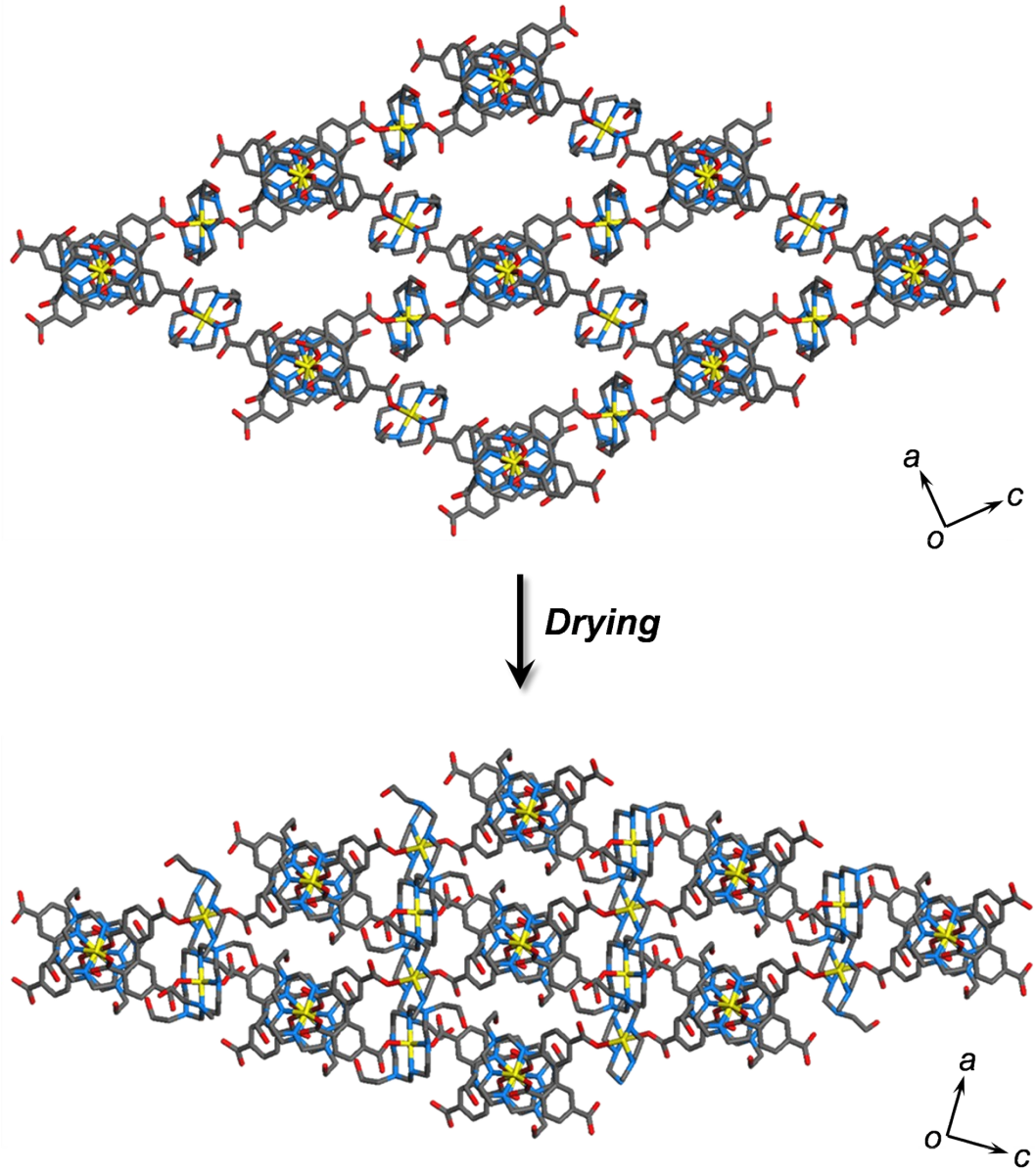

Figure S5. Comparison of SCD structures of ***as-flex*MOF(OH)** and ***cp-flex*MOF(OH)**, shown in the specific plane. Color scheme: Ni, yellow; C, black; O, red; N, blue.

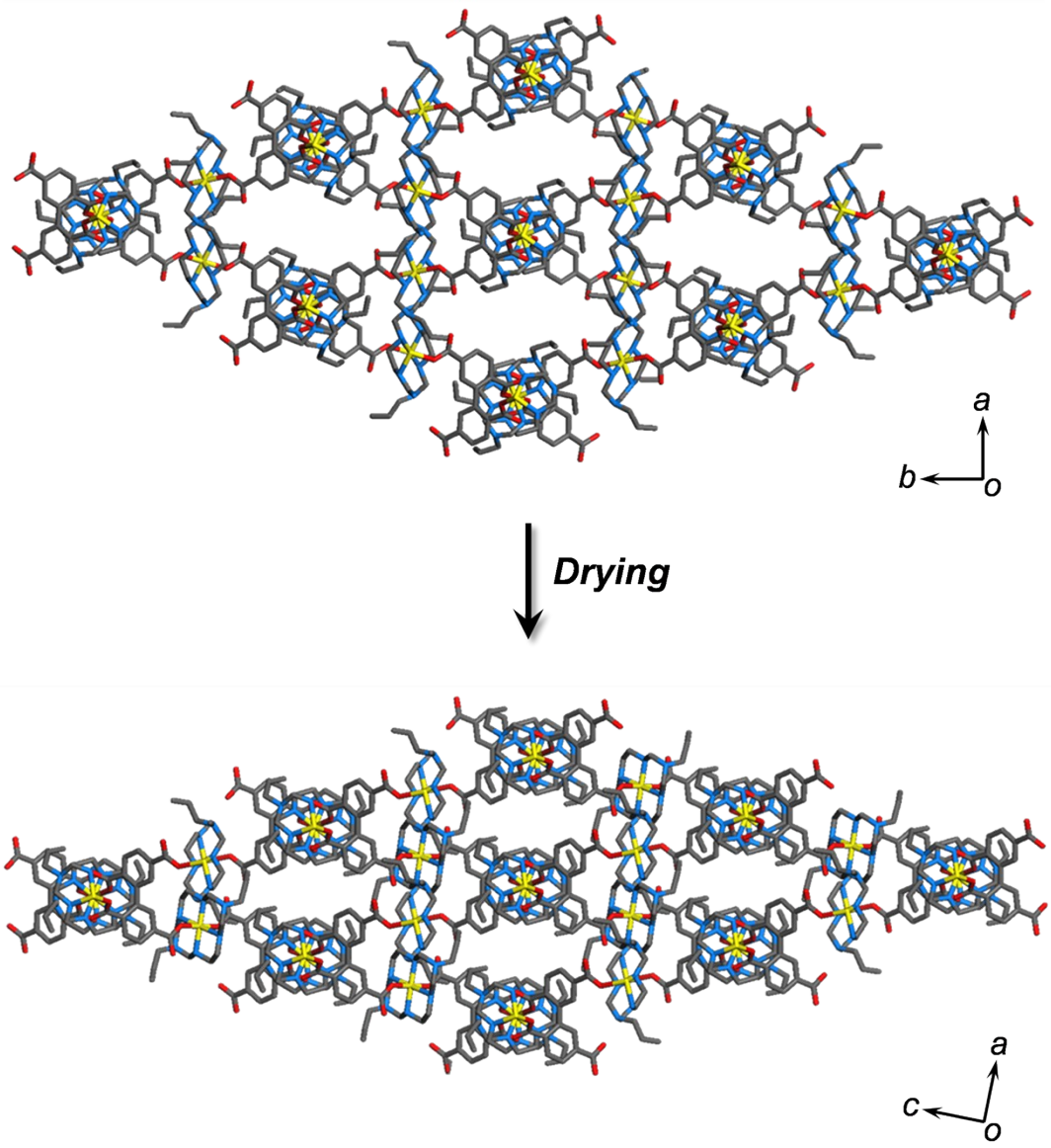

Figure S6. Comparison of SCD structures of ***as-flex*MOF(CH$_2$)** and ***cp-flex*MOF(CH$_2$)**, shown in the specific plane. Color scheme: Ni, yellow; C, black; O, red; N, blue.

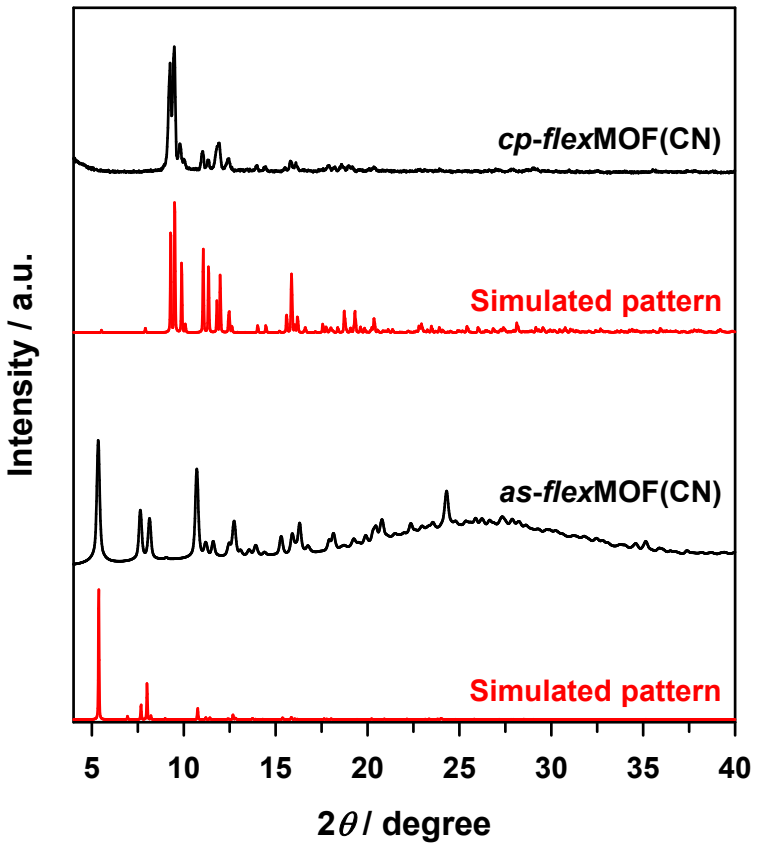

Figure S7. Comparison of XRPD measured (black) and simulated patterns (red) of ***as-flex*MOF(CN)** and ***cp-flex*MOF(CN)**.

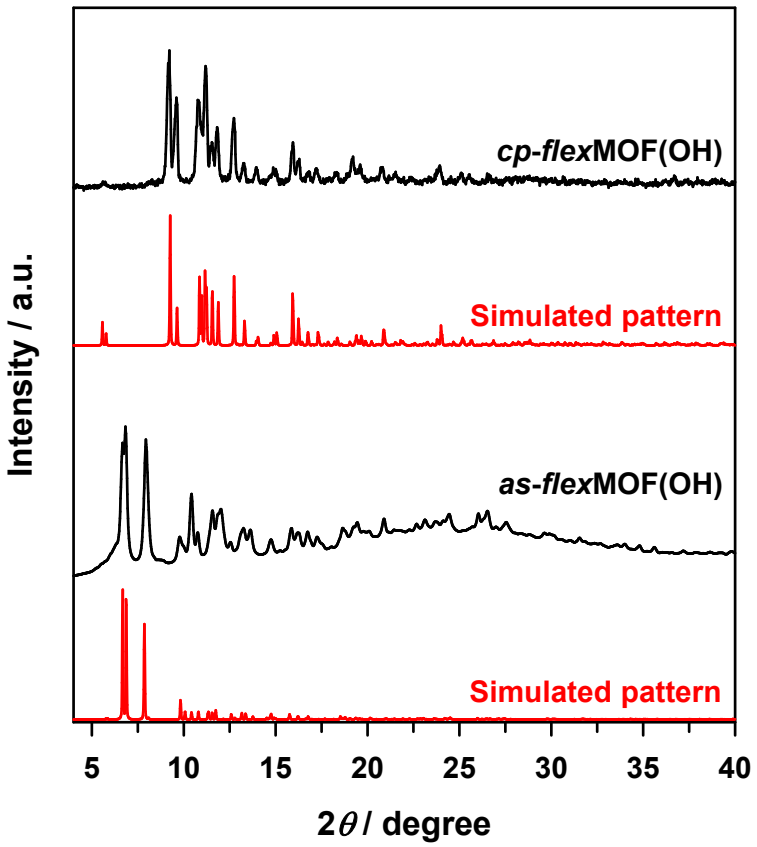

Figure S8. Comparison of XRPD measured (black) and simulated patterns (red) of ***as-flex*MOF(OH)** and ***cp-flex*MOF(OH)**.

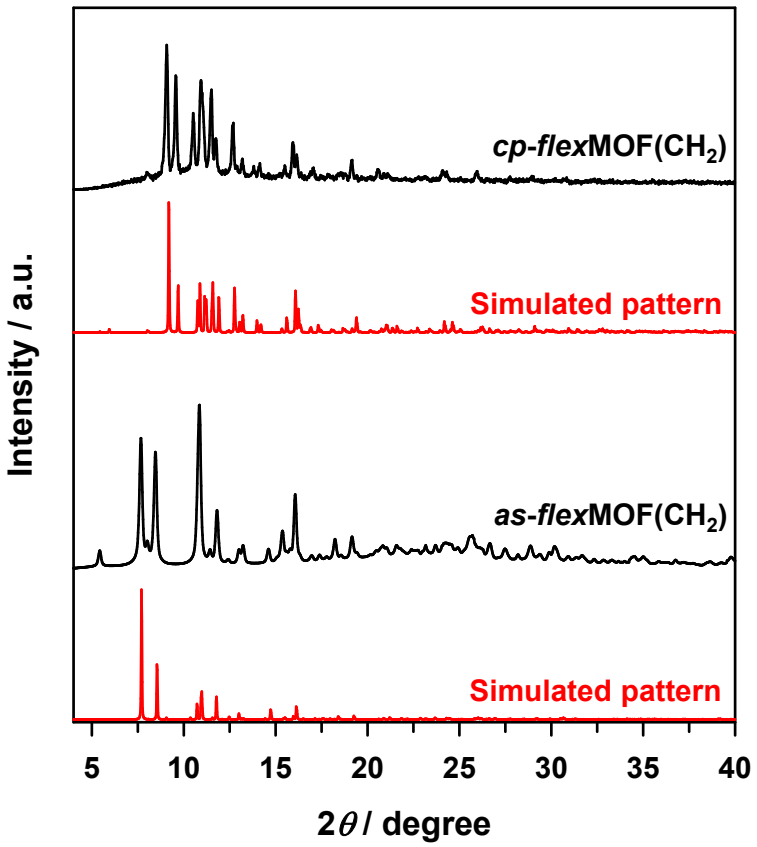

Figure S9. Comparison of XRPD measured (black) and simulated patterns (red) of ***as-flex*MOF(CH$_2$)** and ***cp-flex*MOF(CH$_2$)**.

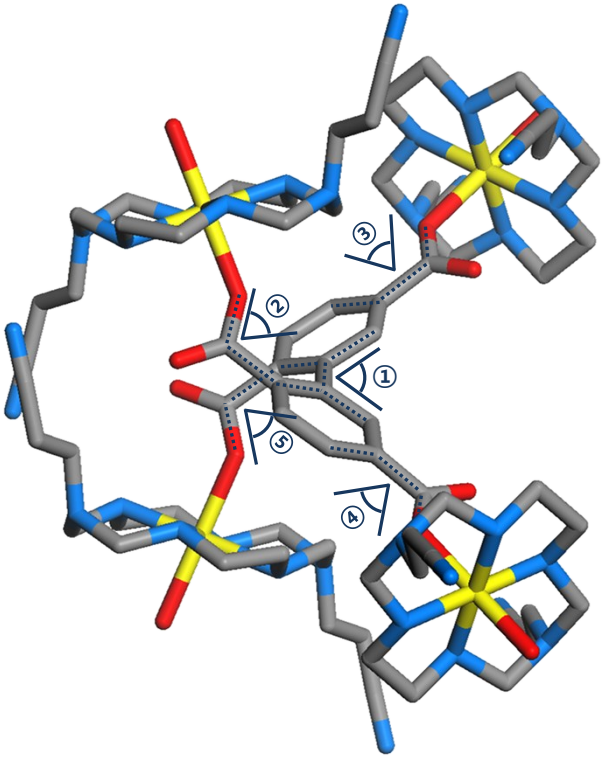

Angle	***as-flex*MOF(CN)**	***cp-flex*MOF(CN)**
①	52.780 º	59.833 º
②	41.868 º	60.063 º
③	13.458 º	9.822 º
④	13.458 º	3.268 º
⑤	41.868 º	39.374 º

Figure S10. Change of dihedral angle in the $BPTC^{4-}$ ligand of ***flex*MOF(CN)** after drying.

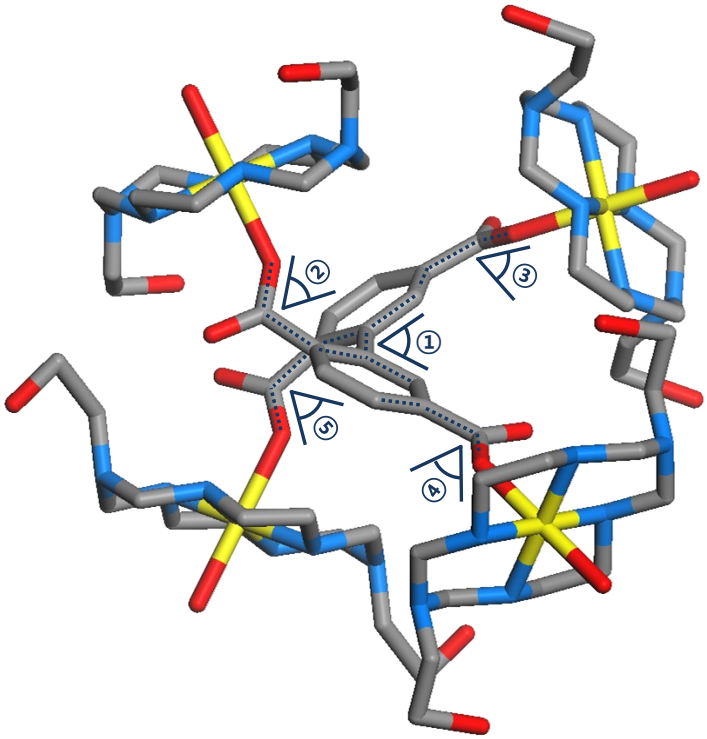

Angle	***as-flex*MOF(OH)**	***cp-flex*MOF(OH)**
①	50.318 º	63.996 º
②	46.676 º	37.849 º
③	6.411 º	14.276 º
④	13.339 º	17.977 º
⑤	39.126 º	59.446 º

Figure S11. Change of dihedral angle in the $BPTC^{4-}$ ligand of ***flex*MOF(OH)** after drying.

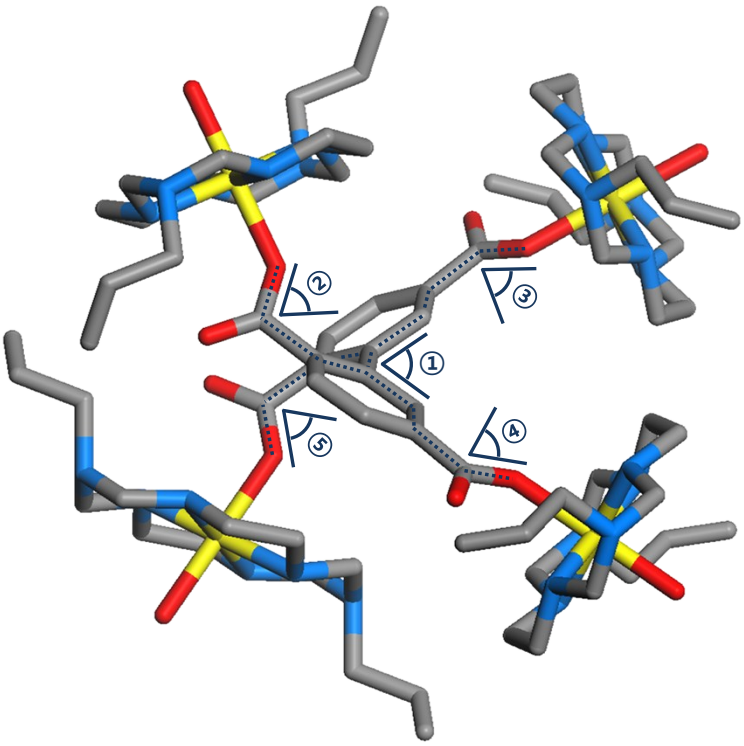

Angle	***as-flex*MOF(CH_2)**	***cp-flex*MOF(CH_2)**
①	57.267 º	57.681 º
②	48.630 º	46.196 º
③	13.475 º	15.847 º
④	10.707 º	-8.641 º
⑤	45.549 º	42.703 º

Figure S12. Change of dihedral angle in the $BPTC^{4-}$ ligand of ***flex*MOF(CH_2)** after drying.

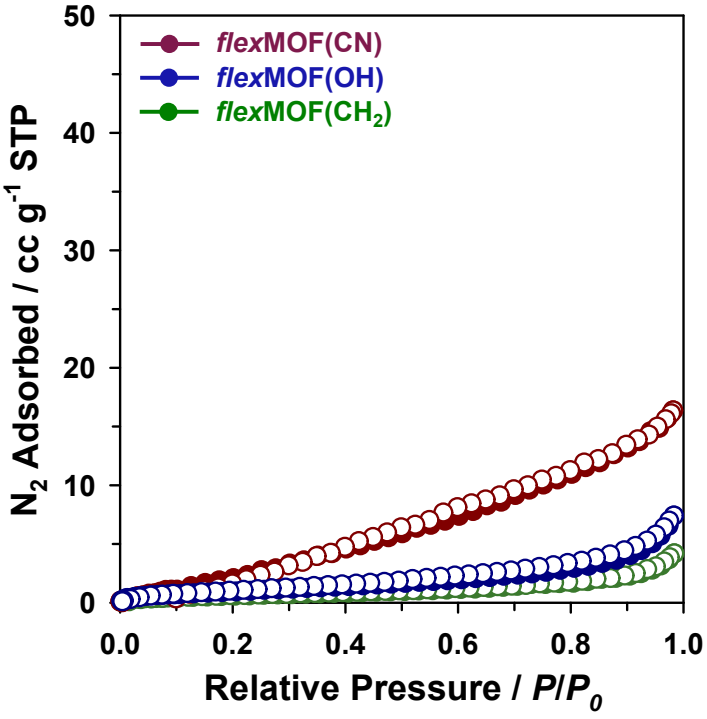

Figure S13. N_2 sorption isotherms of ***flex*MOF(CN)**, ***flex*MOF(OH)**, and ***flex*MOF(CH_2)** at 77 K.

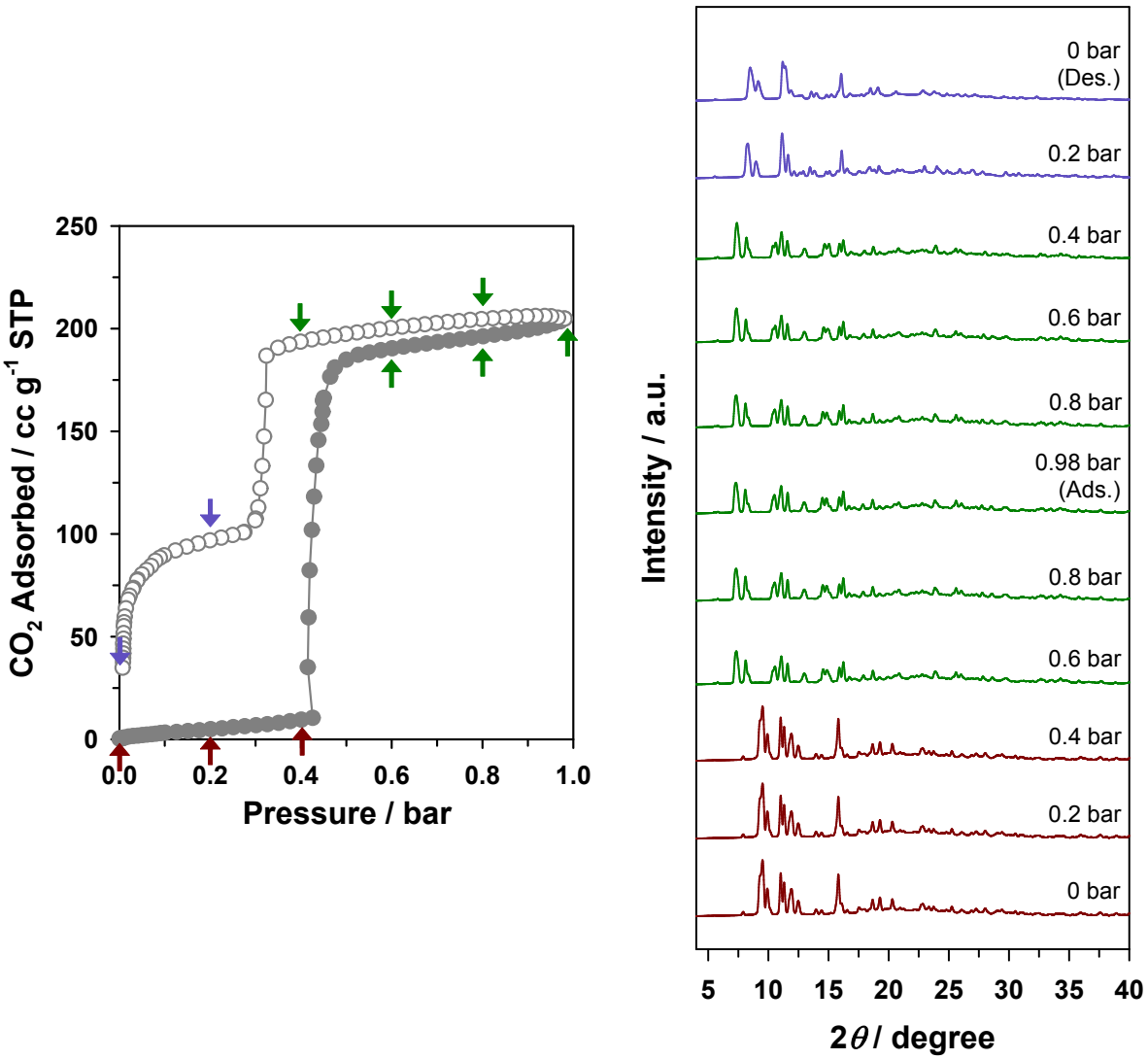

Figure S14. CO_2 adsorption/desorption isotherm of ***flex*MOF(CN)** and *in-situ* XRPD experimental results at 196 K.

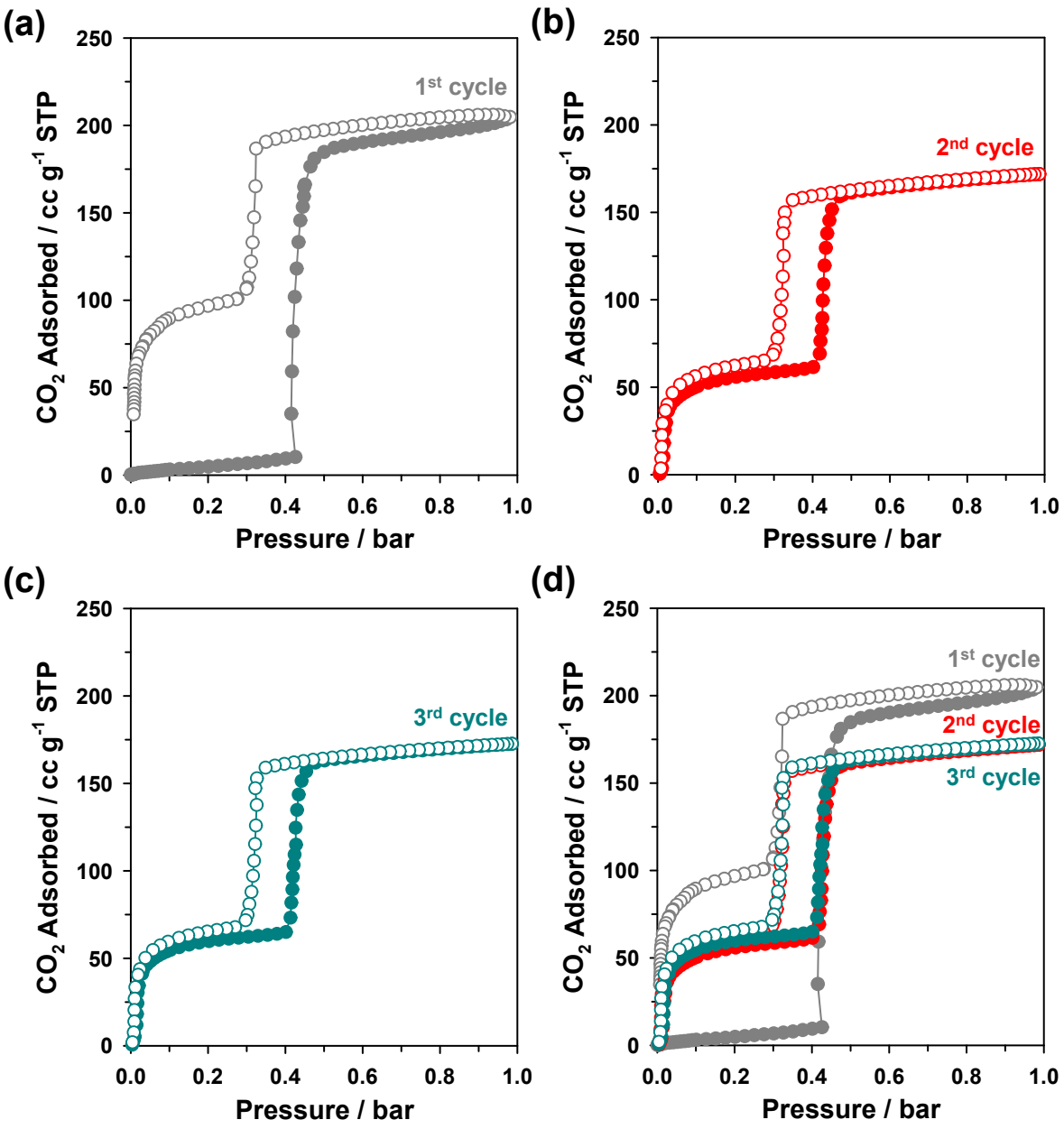

Figure S15. The consecutive cycle cycles of CO_2 adsorption/desorption isotherms of ***flex*MOF(CN)** at 196 K.

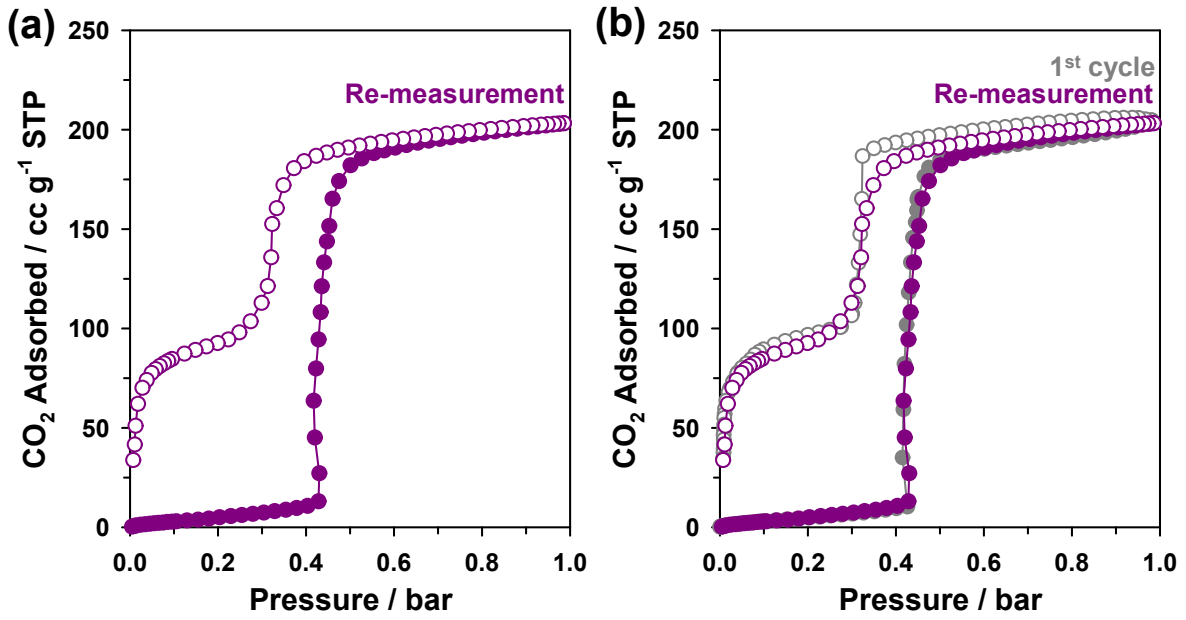

Figure S16. (a) CO_2 re-adsorption/desorption isotherm of ***flex*MOF(CN)** at 196 K after re-activation by heating under vacuum.

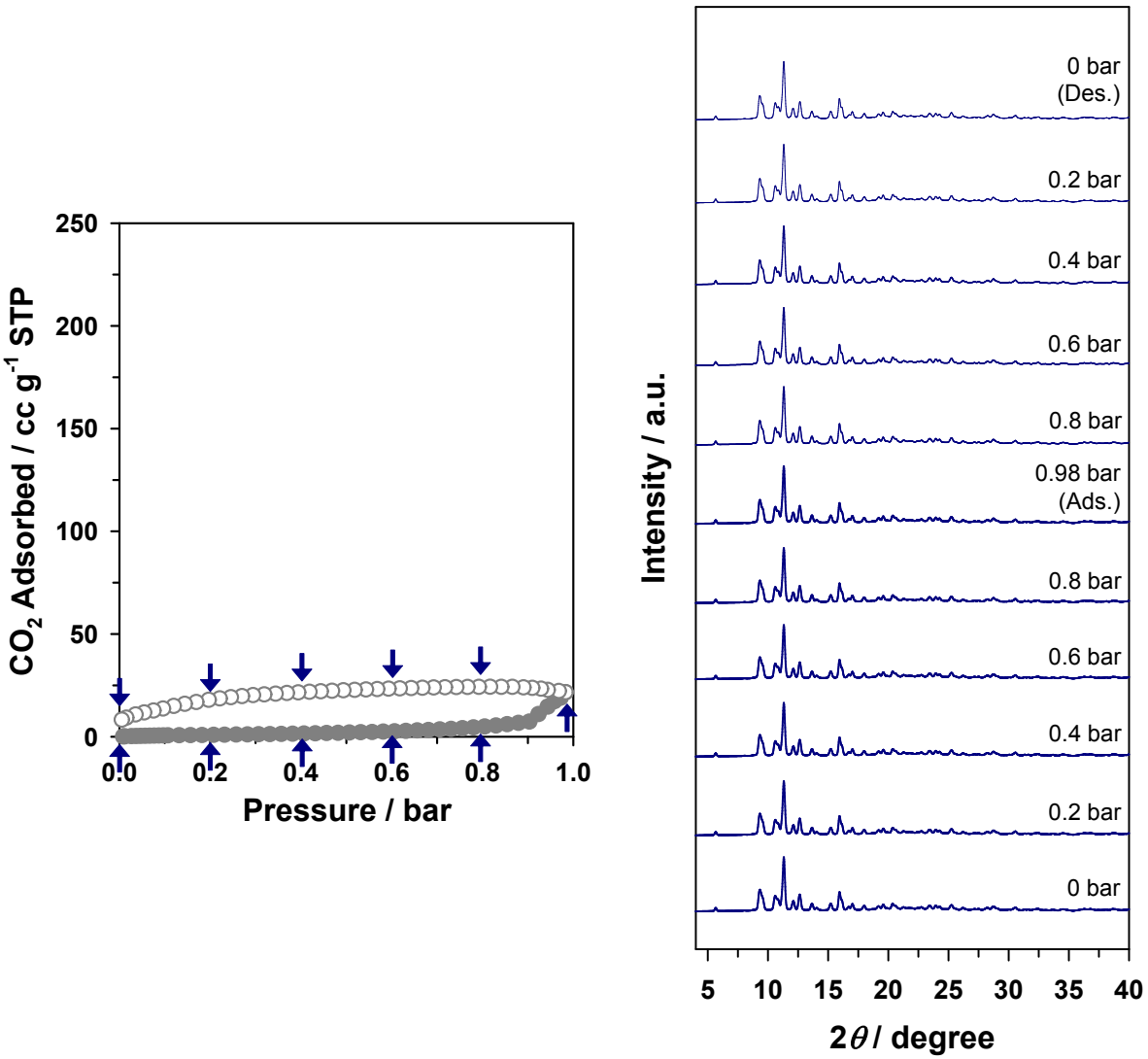

Figure S17. CO_2 adsorption/desorption isotherm of ***flex*MOF(OH)** and *in-situ* XRPD experimental results at 196 K.

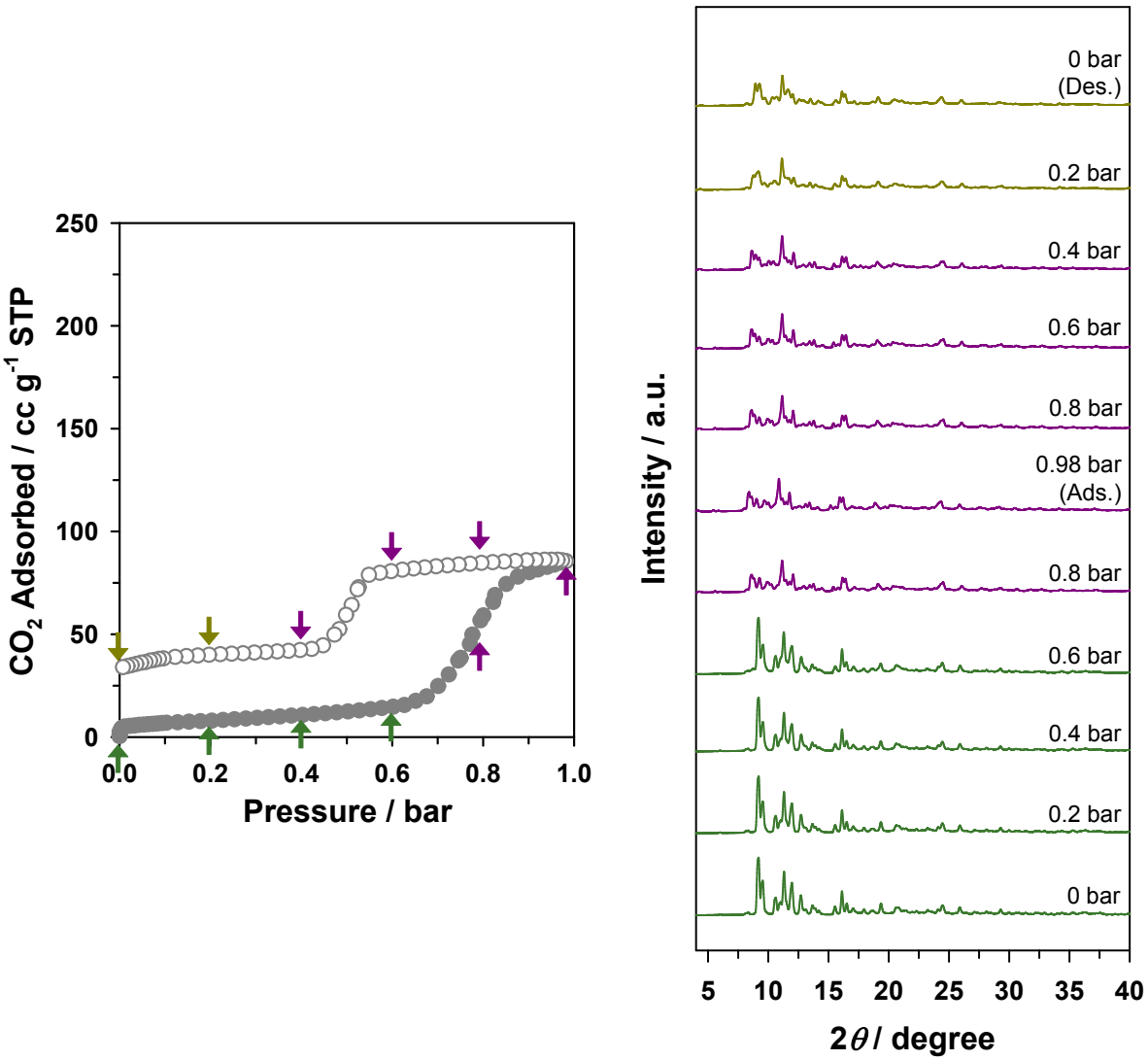

Figure S18. CO_2 adsorption/desorption isotherm of ***flex*MOF(CH_2)** and *in-situ* XRPD experimental results at 196 K.

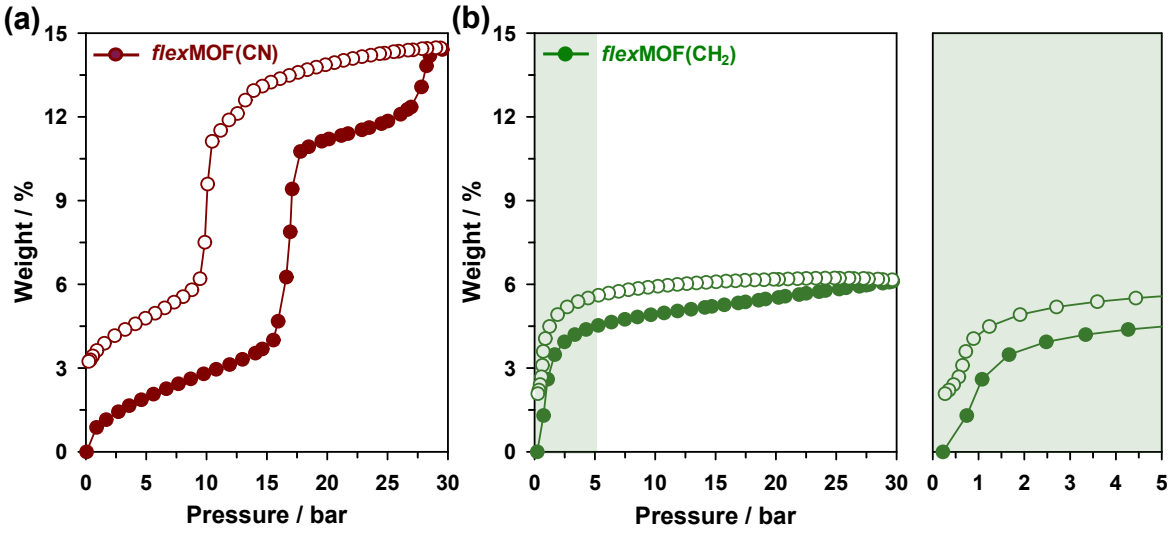

Figure S19. (a) CO_2 adsorption/desorption isotherm of ***flex*MOF(CN)** at 298 K. (b) CO_2 adsorption/desorption isotherm of ***flex*MOF(CH_2)** at 298 K and its expanded graph from 0 to 5 bar.

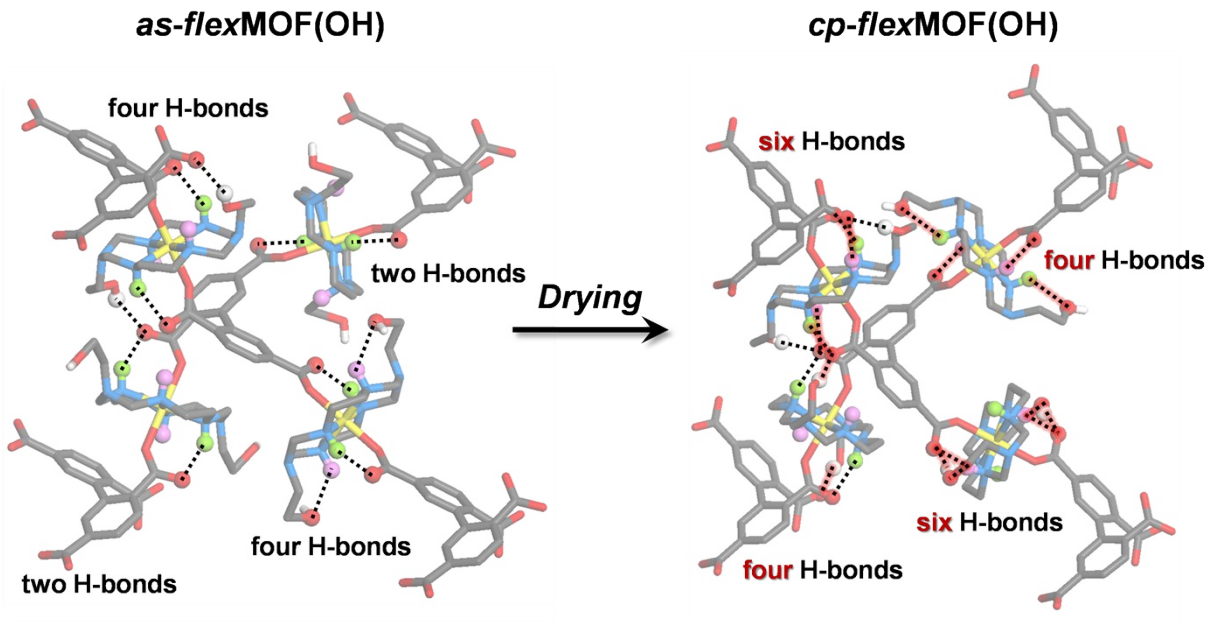

Figure S20. Comparison of SCD structures of ***as-flex*MOF(OH)** and ***cp-flex*MOF(OH)**. Each macrocycles of Ni metal center are stabilized by the hydrogen bond between the carboxylate oxygen of the ligand, the secondary amine hydrogen in the macrocycle, and the oxygen and hydrogen of terminal hydroxyl group. Color scheme: Ni, yellow; C, black; O, red; N, blue; H, white.

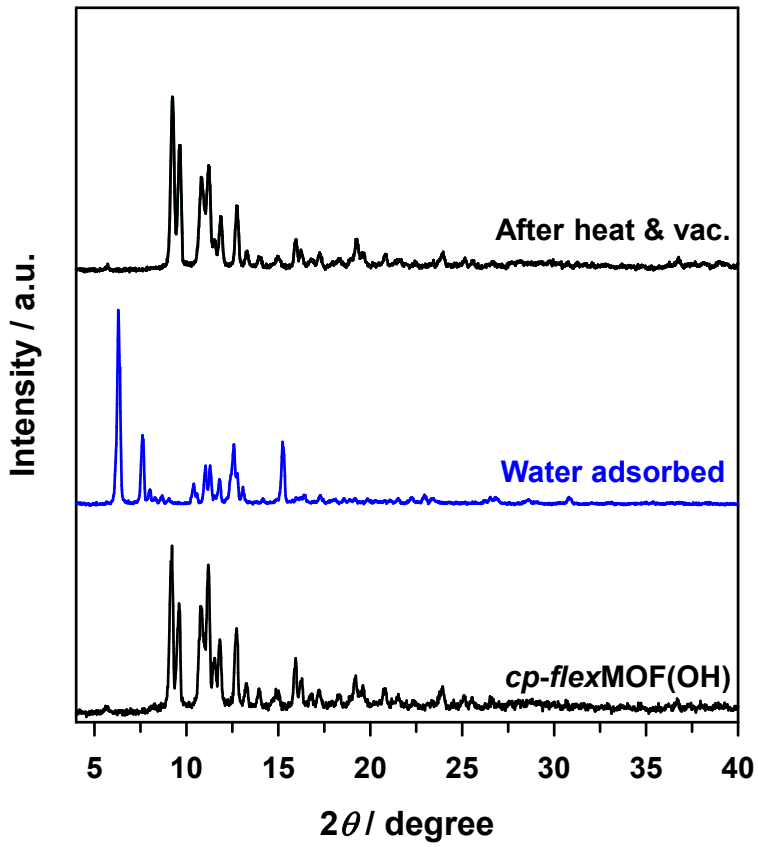

Figure S21. Comparison of XRPD patterns of ***cp-flex*MOF(OH)**, the sample after water adsorption at 298 K, and after re-activation by heating under vacuum.

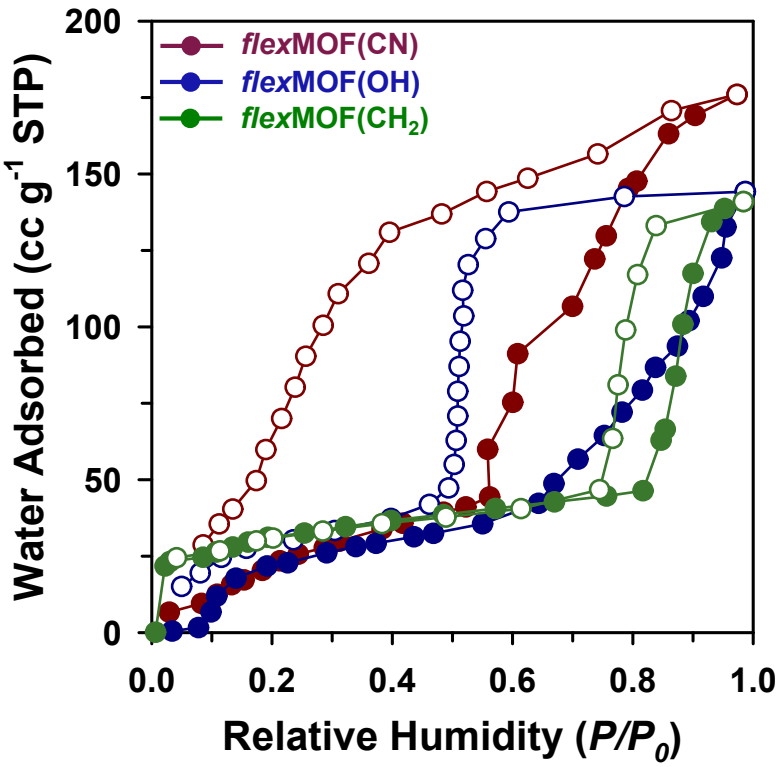

Figure S22. Water vapour isotherms of ***flex*MOF(CN)**, ***flex*MOF(OH)**, and ***flex*MOF(CH_2)** at 298 K.

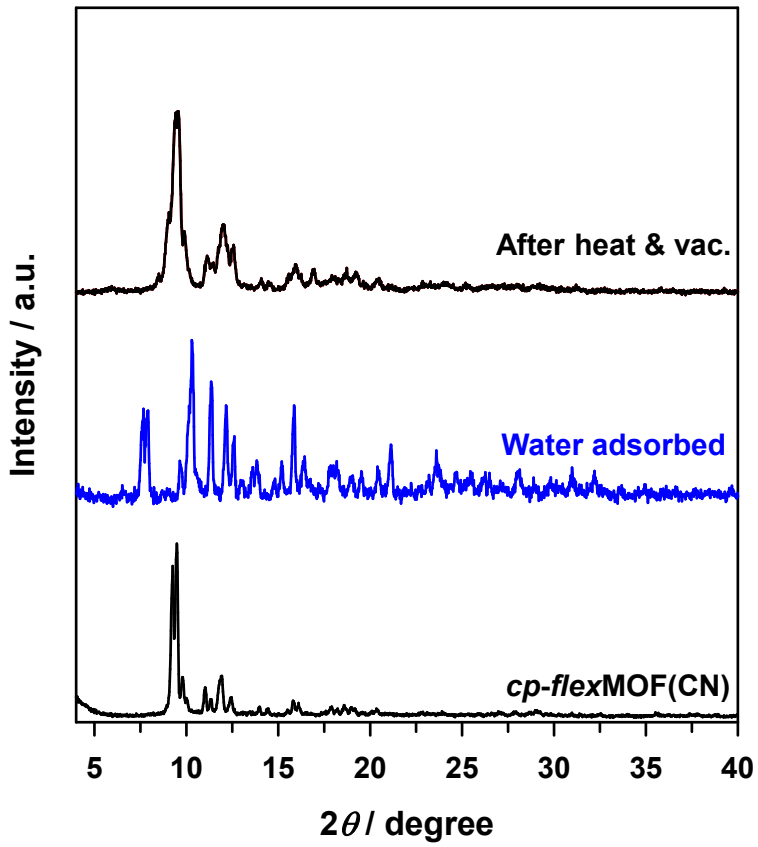

Figure S23. Comparison of XRPD patterns of ***cp-flex*MOF(CN)**, the sample after water adsorption at 298 K, and after re-activation by heating under vacuum.

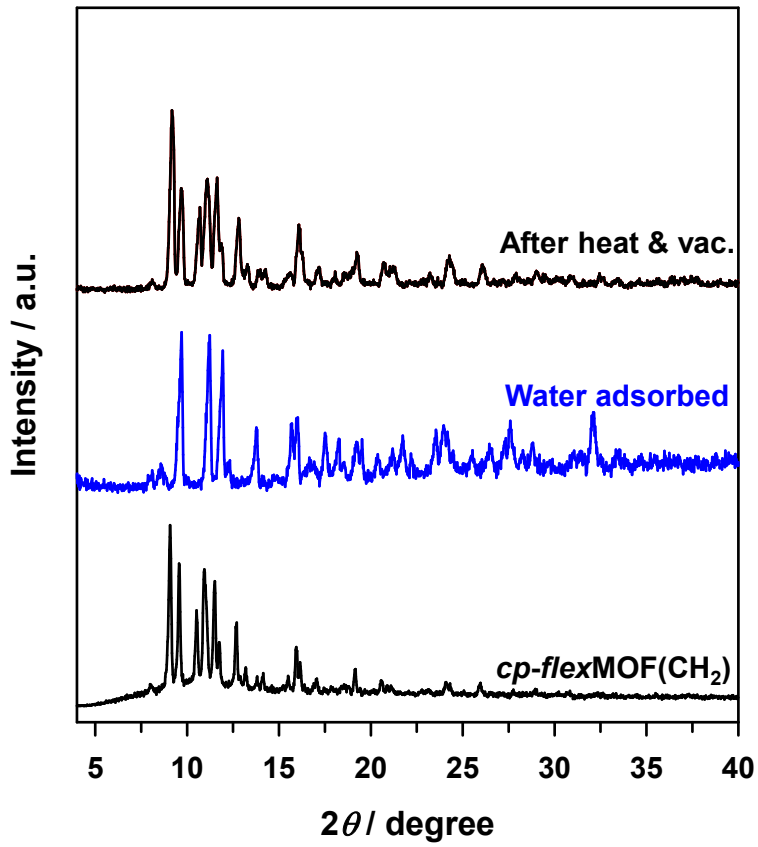

Figure S24. Comparison of XRPD patterns of ***cp-flex*MOF(CH_2)**, the sample after water adsorption at 298 K, and after re-activation by heating under vacuum.

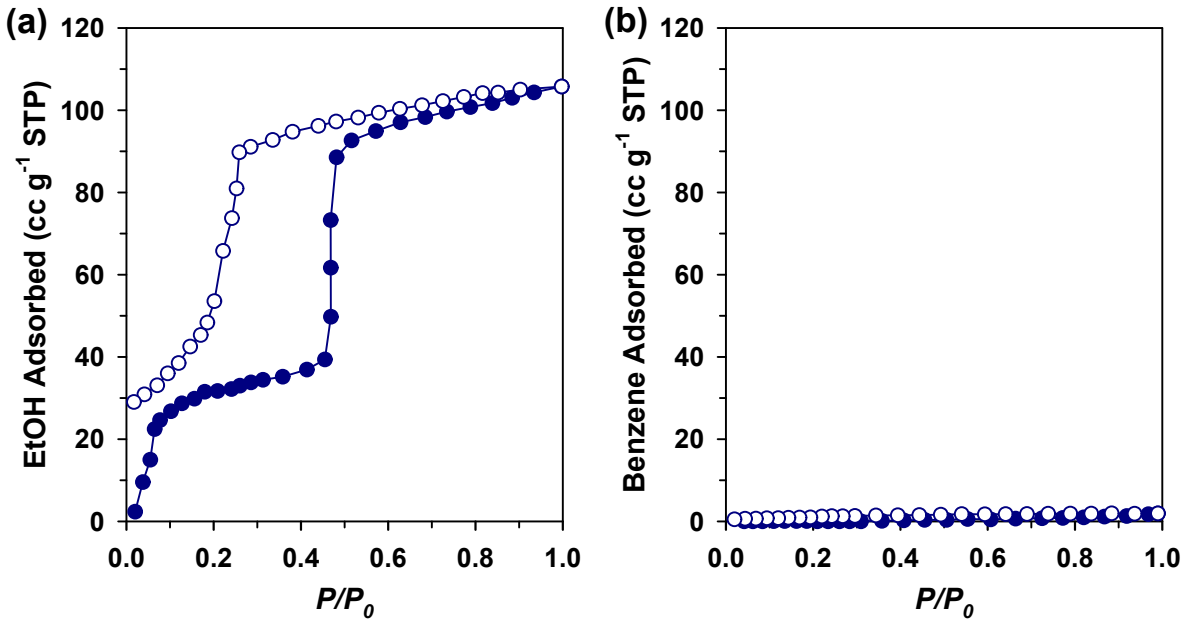

Figure S25. (a) Methanol and (b) benzene vapour sorption isotherms of ***flex*MOF(OH)** at 298 K.

(S1) Holy, P.; Sehnal, P.; Tichy, M.; Zavada, J.; Cisarova, I. *Tetrahedron:Asymmetry*. **2003**, *14*, 245-253.

(S2) Suh, M. P.; Shim, B. Y.; Yoon, T.-S. *Inorg. Chem.* **1994**, *33*, 5509-5514.

(S3) Shin, J. W.; Eom, K.; Moon D. *J. Synchrotron Rad.* **2016**, *23*, 369-373.

(S4) Fit2D program:Andy Hammersley (E-mail: hammersley@esrf.fr), ESRF; 6 RUE JULES HOROWITZBP 22038043 GRENOBLE CEDEX 9FRANCE

(S5) Otwinowski, Z.; Minor, W.; Carter Jr, C. W.; Sweet (Eds.), R. M. Methods in Enzymology 276 Part A; Academic Press: New York, 1997; 307-326.

(S6) Sheldrick, G. M. *Acta Cryst.* **2015**, *A71*, 3-8.

(S7) Sheldrick, G. M. *Acta Cryst.* **2015**, *C71*, 3-8.

(S8) Spek, A. L. *Acta Cryst.* **2015**, *D65*, 148-155.

(S9) Dubbeldam, D.; Calero, S.; Ellis, D. E.; Snurr, R. Q. *Mol. Simul.* **2016**, *42*, 81-101.

(S10) Potoff, J. J.; Siepmann, J. I. *AIChE J.* **2001**, *47*, 1676-1682.